26 January 2007 | $10

Science

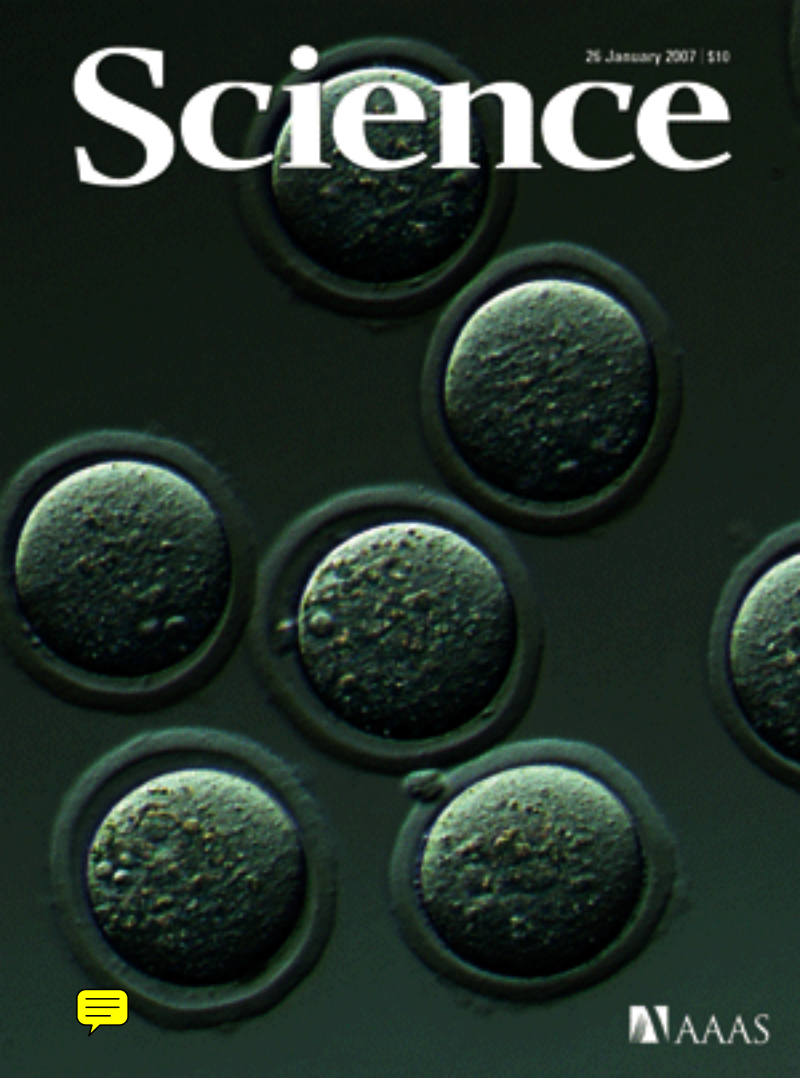

AAAS

Science
AAAS

Histocompatible Embryonic Stem Cells by Parthenogenesis

Kitai Kim, *et al.*

Science **315**, 482 (2007);
DOI: 10.1126/science.1133542

This copy is for your personal, non-commercial use only.

If you wish to distribute this article to others, you can order high-quality copies for your colleagues, clients, or customers by clicking here.

Permission to republish or repurpose articles or portions of articles can be obtained by following the guidelines here.

The following resources related to this article are available online at www.sciencemag.org (this information is current as of May 13, 2010):

Updated information and services, including high-resolution figures, can be found in the online version of this article at:
http://www.sciencemag.org/cgi/content/full/315/5811/482

Supporting Online Material can be found at:
http://www.sciencemag.org/cgi/content/full/1133542/DC1

This article **cites 21 articles**, 8 of which can be accessed for free:
http://www.sciencemag.org/cgi/content/full/315/5811/482#otherarticles

This article has been **cited by** 40 article(s) on the ISI Web of Science.

This article has been **cited by** 7 articles hosted by HighWire Press; see:
http://www.sciencemag.org/cgi/content/full/315/5811/482#otherarticles

This article appears in the following **subject collections**:
Development
http://www.sciencemag.org/cgi/collection/development

Downloaded from www.sciencemag.org on May 13, 2010

Science (print ISSN 0036-8075; online ISSN 1095-9203) is published weekly, except the last week in December, by the American Association for the Advancement of Science, 1200 New York Avenue NW, Washington, DC 20005. Copyright 2007 by the American Association for the Advancement of Science; all rights reserved. The title *Science* is a registered trademark of AAAS.

Histocompatible Embryonic Stem Cells by Parthenogenesis

Kitai Kim,[1,2,4] Paul Lerou,[1,4,5] Akiko Yabuuchi,[1,2,4] Claudia Lengerke,[1,2,4] Kitwa Ng,[1,2,4] Jason West,[1,2,4] Andrew Kirby,[6] Mark J. Daly,[6] George Q. Daley[1,2,3,4]*

Genetically matched pluripotent embryonic stem (ES) cells generated via nuclear transfer or parthenogenesis (pES cells) are a potential source of histocompatible cells and tissues for transplantation. After parthenogenetic activation of murine oocytes and interruption of meiosis I or II, we isolated and genotyped pES cells and characterized those that carried the full complement of major histocompatibility complex (MHC) antigens of the oocyte donor. Differentiated tissues from these pES cells engrafted in immunocompetent MHC-matched mouse recipients, demonstrating that selected pES cells can serve as a source of histocompatible tissues for transplantation.

Parthenogenesis entails the development of an embryo directly from an oocyte without fertilization. Many animal and plant species reproduce via parthenogenesis, but in mice, parthenogenetic embryos develop only to the early limb bud stage because mammalian embryonic development requires gene expression from the paternal genome. Parthenogenetic embryonic stem (pES) cells have been isolated from parthenogenetic blastocysts of mice and primates (*1*, *2*). Both mouse and primate pES cells undergo extensive differentiation in vitro (*2*, *3*), and pES cells contribute widely to adult tissues in chimeric mice (*1*). A human case of parthenogenetic chimerism has been described in which the hematopoietic system and skin were derived from parthenogenetic cells (*4*). In addition to pluripotent stem cells from fertilized embryos and embryos created by somatic-cell nuclear transfer (*5*), parthenogenesis is another method for creating pluripotent stem cells that might serve as a source of tissue for transplantation.

Highly efficient methods of experimental murine parthenogenesis exist in which oocytes arrested at the second meiotic metaphase (MII) are chemically activated in the presence of cytochalasin, a drug that prevents extrusion of the second polar body (*6*). Diploidy is maintained, and the resulting pseudozygote can develop into a blastocyst from which ES cells can be isolated [which we term p(MII)ES cells (*7*)]. In some cases, pES cells harbor a duplication of a haploid genome and are thus believed to be predominantly homozygous (*7*, *8*). Because tissues derived from homozygous pES cells would express only one of two sets of parental histocompatibility antigens, they can be more readily matched to patients and might pose less risk of tissue rejection (*9*). However, in heterozygous recipients, major histocompatibility complex (MHC) homozygous tissues may be rejected by natural killer (NK) cells that recognize the lack of one set of histocompatibility antigens, a phenomenon called "hybrid resistance" that is particularly relevant to bone marrow transplantation (*10*). As compared with mismatched organs, partial MHC antigen matching enhances allograft survival, but full MHC-matched tissues are the most favorable for transplant (*11*). The only certain strategy for avoiding immunologic complications is to transplant genetically identical tissues, but this limits transplantation to autologous tissues, transplants between monozygotic twins, or cells created by somatic cell nuclear transfer.

Here we characterize pluripotent ES cell lines generated by parthenogenesis in which both of the maternal MHC loci have been maintained. Differentiated tissues from such MHC-matched ES cells can be transplanted into the oocyte donor strain without rejection, suggesting that these cells could be a favorable source of histocompatible tissues for transplantation.

Recombinant MHC-matched p(MII)ES cells. We reasoned that during the isolation of p(MII)ES cells from hybrid F_1 mice, recombination events occurring between paired homologous chromosomes in meiosis I would produce cells that had restored heterozygosity at the MHC loci (Fig. 1B). Recombination frequencies place the murine H-2 MHC locus at ~18.5 centimorgans (cM) from the centromere on mouse chromosome 17 (*12*), thus predicting that approximately one

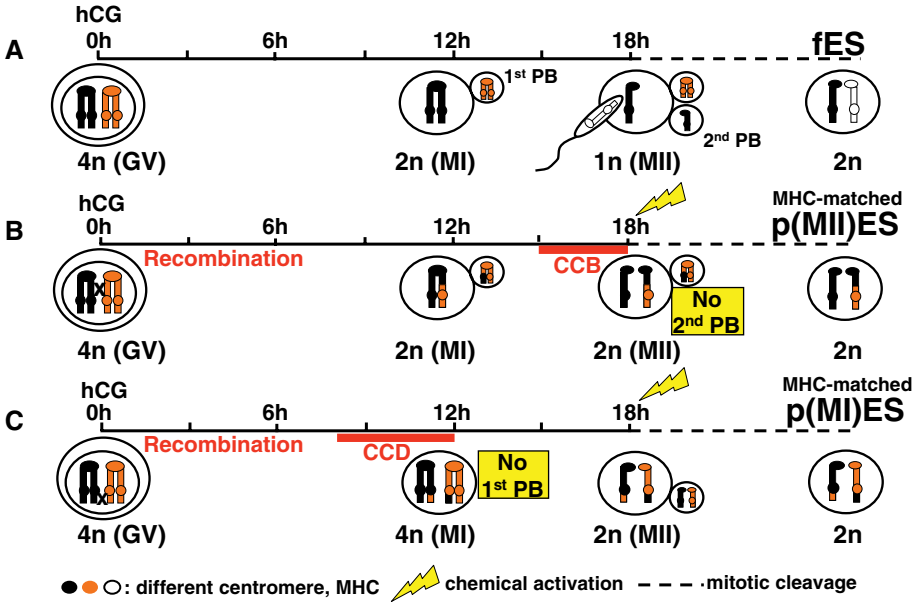

Fig. 1. Chromosome dynamics during normal and artificial murine oocyte maturation. (**A**) Normal fertilization. Immature oocytes arrested at diplotene of the first meiotic prophase harbor 20 sets of paired homologous chromosomes (bivalents). A single bivalent pair is illustrated at left, without recombination. The maternal or paternal chromosomes segregate into the first polar body (1st PB) during MI. At fertilization, half of the chromosomes are extruded via the second polar body (2nd PB), and the incoming sperm restores the diploid chromosome complement. Blastocysts derived by fertilization yield fES cells. hCG, human chorionic gonadotropin. GV, germinal vesicle. Timeline is shown at top; h, hours. (**B**) Parthenogenetic oocyte maturation. MII-arrested oocytes are activated in cytochalasin B, blocking extrusion of the second polar body. Diploidy is maintained and the resulting blastocysts yield p(MII)ES cells. Recombination events produce MHC-matched p(MII)ES cells. (**C**) Parthenogenetic activation of immature oocytes (*16*). Inhibiting extrusion of the first polar body prevents segregation of the homologous chromosome pairs. Extrusion of a polar body restores diploidy.

[1]Division of Pediatric Hematology/Oncology, Children's Hospital Boston and Dana Farber Cancer Institute, Boston, MA 02115, USA. [2]Department of Biological Chemistry and Molecular Pharmacology, Harvard Medical School, Boston, MA 02115, USA. [3]Division of Hematology, Brigham and Women's Hospital, Boston, MA 02115, USA. [4]Harvard Stem Cell Institute, Cambridge, MA 02138, USA. [5]Division of Newborn Medicine, Brigham and Women's Hospital and Children's Hospital, Harvard Medical School, Boston, MA 02115, USA. [6]Center for Human Genetic Research, Massachusetts General Hospital, Boston, MA 02115, USA.

*To whom correspondence should be addressed. E-mail: george.daley@childrens.harvard.edu

Downloaded from www.sciencemag.org on May 13, 2010

in five meioses will yield a crossover event. We collected mature oocytes from C57BL/6 × CBA F_1 mice and initiated parthenogenetic embryo development via a protocol that prevents extrusion of the second polar body. From the 74% of activated oocytes that developed to blastocysts, we isolated 72 p(MII)ES cell lines (Table 1).

We used polymerase chain reaction (PCR) amplification followed by allele-specific restriction enzyme digestion or direct sequencing of single-nucleotide polymorphisms (SNPs) within the H-2 region of chromosome 17 to determine whether recombination had restored heterozygosity at the MHC loci (*13*). 24 out of 72 p(MII) ES cells (33%) harbored the heterozygous MHC genotype of the oocyte donor (fig. S1A, black circles; and fig. S1, B and C). Genotyping of flanking markers on chromosome 17 confirmed the MHC heterozygosity in a subset of eight selected cell lines (fig. S1C). We call ES cells selected in this manner recombinant MHC-matched p(MII)ES cells.

Recombinant MHC-matched p(MII)ES cells were differentiated into embryoid bodies (EBs) for 14 days, followed by culture on gelatin-coated tissue culture plates for an additional 14 days in order to examine MHC antigen expression on a differentiated population of epithelial-like cells (*14*). Differentiated p(MII)ES cells that had not recombined at the MHC loci by polymorphism analysis expressed only one of the parental MHC proteins ($H2K^b$ for C57BL/6 mice; Fig. 2B), whereas MHC-matched p(MII)ES cells that had recombined expressed both $H2K^b$ and $H2K^k$ on all cells (Fig. 2C). These data confirm the heterozygous genotype by MHC antigen expression. A majority of p(MII)ES cells had a normal karyotype (fig. S2A; n = 16 normal karyotypes out of 19 lines tested). A minority of p(MII)ES cells showed the loss of one X chromosome, a phenomenon known to occur in female ES cells (*15*).

MHC-matched p(MI)ES cells. In a second method aimed at generating genetically matched pES cells from C57BL/6 × CBA F_1 mice, we induced parthenogenetic development of immature oocytes while interfering with the segregation of the paired homologous chromosomes during the first meiotic metaphase (MI; Fig. 1C). This protocol has been reported to yield parthenogenetic embryos that are genetic clones of the oocyte donor by preventing segregation of the homologous maternal and paternal chromosomes (*16*). From the 56% of activated oocytes that developed into blastocysts, we isolated 23 ES cell lines, which we term p(MI)ES cells (Table 1). We determined the genotypes of the MHC region of the p(MI)ES cell lines by PCR amplification followed by allele-specific restriction enzyme digestion or direct sequencing of SNP loci on chromosome 17, and we observed MHC heterozygosity in 21 of 23 cell lines (fig. S1A, white circles; and fig. S3). Genotyping of flanking markers on chromosome 17 confirmed the heterozygous MHC genotype and MHC identity with the oocyte donor in 10 members of a selected set of 12 p(MI)ES cell lines (fig. S1C).

MHC-matched p(MI)ES cells were differentiated for 28 days in culture as described above and examined by flow cytometry. The differentiated derivatives expressed both $H2K^b$ and $H2K^k$ on all cells, confirming heterozygosity of the MHC locus by surface protein expression (Fig. 2D). In seven p(MI)ES cell lines, we documented a normal diploid chromosome content by direct chromosome counting (fig. S2C). Seven p(MI)ES cell lines had 39 chromosomes, reflecting the tendency of female ES cells to lose an X chromosome (*7*, *15*). Nine lines showed variable chromosome content. A more detailed genomic analysis that distinguishes these diploid and aneuploid classes of p(MI)ES cells is presented below.

Pericentromeric genotype and patterns of recombination in p(MII) and p(MI)ES cells. To assess the pattern of chromosomal segregation observed under the different oocyte activation protocols and to determine the degree of genetic identity of the pES cells with the oocyte donor, we determined the pericentromeric genotype and distal recombination of the p(MII)ES and p(MI)ES cell lines using SNPs that distinguish the parental mouse strains (C57BL/6 and CBA) (*17*). We hypothesized that p(MII)ES cells would be predominantly homozygous, with recombination reflected by a telomeric predominance of heterozygous SNPs. Conversely, we reasoned that the p(MI)ES cells would be predominantly heterozygous, with recombination reflected by a telomeric predominance of homozygous SNPs. Moreover, ES cells isolated from embryos that resulted from natural fertilization events between strains of inbred mice (fES cells from F_1 matings) should show heterozygosity at

Table 1. Parthenogenetic oocyte activation and ES cell derivation from a C57BL/6 × CBA F_1 mouse. Numbers indicate embryos reaching a given stage/total oocytes.

	Efficiency of p(MII)ES cell derivation					
Stage	**1 cell**	**2 cells**	**4 cells**	**Morula**	**Blastocyst**	**p(MII)ES cells**
Rate of development	150/150 (100%)	125/150 (83%)	117/150 (78%)	115/150 (77%)	111/150 (74%)	72/111 (65%)
	Efficiency of p(MI)ES cell derivation					
Rate of development	112/112 (100%)	87/112 (78%)	81/112 (72%)	75/112 (67%)	63/150 (56%)	23/63 (37%)

Table 2. Teratoma formation after injection of differentiated fES, p(MII)ES, and p(MI)ES cells into MHC-matched and -mismatched recipients, observed for 3 months. $Rag2^{-/-}/\gamma c^{-/-}$ mice are on the C57BL/6 background. Numbers represent teratomas formed/total mice injected. ($P < 0.001$ for the hypothesis that haploidentity or full MHC match predicts teratoma formation; see methods in supporting online material for assumptions in statistical analysis.)

	ES cell type (MHC)					
Recipient mouse	**fES cells (C57BL/6)**	**fES cells (CBA)**	**fES cells (C57BL/6 × CBA)**	**p(MII)ES cells (C57BL/6)**	**p(MII)ES cells (C57BL/6 × CBA)**	**p(MI)ES cells (C57BL/6 × CBA)**
$Rag2^{-/-}/\gamma c^{-/-}$	+ (4/4)	+ (5/5)	+ (2/3)	+ (4/4)	+ (3/3)	+ (3/3)
CBA	− (0/4)	+ (5/5)	− (0/3)	− (0/3)	− (0/4)	− (0/4)
C57BL/6	+ (5/7)	− (0/5)	− (0/5)	+ (8/12)	− (0/5)	− (0/5)
C57BL/6 × CBA F_1	+ (3/5)	+ (3/5)	+ (6/8)	+ (12/12)	+ (4/5)	+ (5/5)

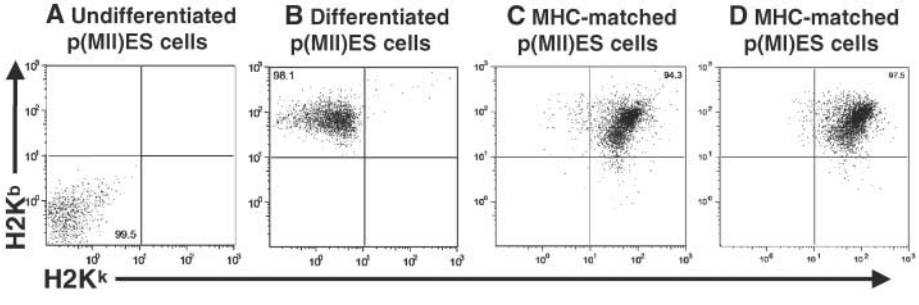

Fig. 2. MHC protein expression on pES cells. Flow cytometric detection of H2K protein expression is shown on (**A**) undifferentiated p(MII)ES cells, (**B**) differentiated MHC-homozygous p(MII)ES, (**C**) MHC-heterozygous p(MII)ES, and (**D**) MHC-heterozygous p(MI)ES cells.

Downloaded from www.sciencemag.org on May 13, 2010

all loci, because the gametes derive from homozygous parents in which meiotic recombination is genetically invisible. We genotyped three SNPs on chromosome 17 in 72 p(MII)ES, 23 p(MI)ES, and 20 fES cell lines, and a single pericentrimeric SNP on each chromosome in one p(MII)ES and five p(MI)ES cell lines (fig. S4). Based on the results of this low-resolution genotyping, we selected a set of 17 p(MII)ES and 20 p(MI)ES cells and performed higher-resolution genotyping using a standard panel of 768 mouse markers evenly spaced across the genome [an expansion of a previously described SNP set (*18*)]. A total of 514 markers spanning the 2.25 gigabases (Gb) across the 19 autosomes were informative: They were polymorphic between C57BL/6 and CBA and had a control F_1 correctly identified as heterozygous (resulting in an average intermarker distance of 4.6 Mb).

SNP genotyping confirmed the hypothesized patterns of recombination but revealed a surprisingly high degree of heterozygosity for the p(MII)ES cells. Because sister chromatid segregation is prevented in MII, all chromosomes were substantially homozygous near their centromeres for one of the two parental strains (Fig. 3A and figs. S5 and S6). Because of recombination, the heterozygosity of SNP markers increased in frequency in proportion to the genetic distance from the centromere (Fig. 3A, right panel; and fig. S6A). Despite the presumption of predominant homozygosity in p(MII)ES cells, we found homozygosity at only 36.9% of loci in a survey of 17 p(MII)ES cell lines, with a range of homozygosity between 23.9 and 47.5% (fig. S7). These data demonstrate that, contrary to expectation, recombination renders the majority of loci in p(MII)ES cells heterozygous.

Some p(MII)ES cells harbored genotypes that showed homozygosity of SNPs from one parental strain near the centromere, followed by a region of heterozygosity, and then a telomeric region of homozygosity of SNPs from the other parental strain (chromosomes 8 and 10 in Fig. 3A). This pattern is consistent with meiotic recombination between both sister chromatid pairs of homologous chromosomes, which occurs during MI, followed by segregation of the bivalents into separate cells upon extrusion of the first polar body, and then co-segregation of the recombinant sister chromatids into the same cell due to inhibition of extrusion of the second polar body (Fig. 1B). With both sister chromatids undergoing recombination separately, we postulated that p(MII)ES cells, although constrained to be homozygous at the centromeres, would manifest recombination at a rate that would be equivalent to an F_2 intercross between two F_1 mice. We calculated the genetic linkage map from the p(MII)ES genotypes using the program MAPMAKER/EXP version 3 under the model of an F_2 intercross, and across all autosomes we estimated a total map length of 1329 cM. This is broadly consistent with the Massachusetts Institute of Technology/Whitehead map, which reported a total autosomal map length estimate of 1338 cM (*19*).

Analysis of the recombination patterns of 20 p(MI)ES cells showed two distinct subgroups. Twelve of the p(MI)ES cells showed a predominant pattern of heterozygosity beginning at the centromere, followed on some chromosomes by telomeric regions of homozygosity (Fig. 3F and fig. S6B). When the genotype data of these 12 lines were similarly evaluated under the assumption of an F_2 intercross, the observed map length was significantly suppressed (910 cM). Despite the high density of polymorphic markers examined, 94 of the 228 autosomes in these 12 lines were observed to be completely heterozygous (fig. S7). These observations drive the estimated map length down as compared to that of the p(MII)ES cells and a standard F_2 recombination pattern. Indeed, the map length is suppressed because the recombinant chromosomes will in some cases co-segregate by chance (or by nondisjunction) into the same cell, thereby preserving heterozygosity in the genotyping assay (fig. S8).

A subset of eight p(MI)ES cells demonstrated complete heterozygosity across all loci, suggesting genetic identity of the parthenogenetic embryo with the oocyte donor—in effect, a parthenogenetic clone, as originally reported (*16*). However, all of the eight p(MI)ES cell lines that show complete heterozygosity are in fact aneuploid, with a range of chromosome counts between 38 and 77. Thus we speculate that these panheterozygous p(MI)ES cells derive from tetraploid blastocysts that manifest infidelity of chromosomal segregation during derivation and culture. Indeed, when oocytes are activated soon

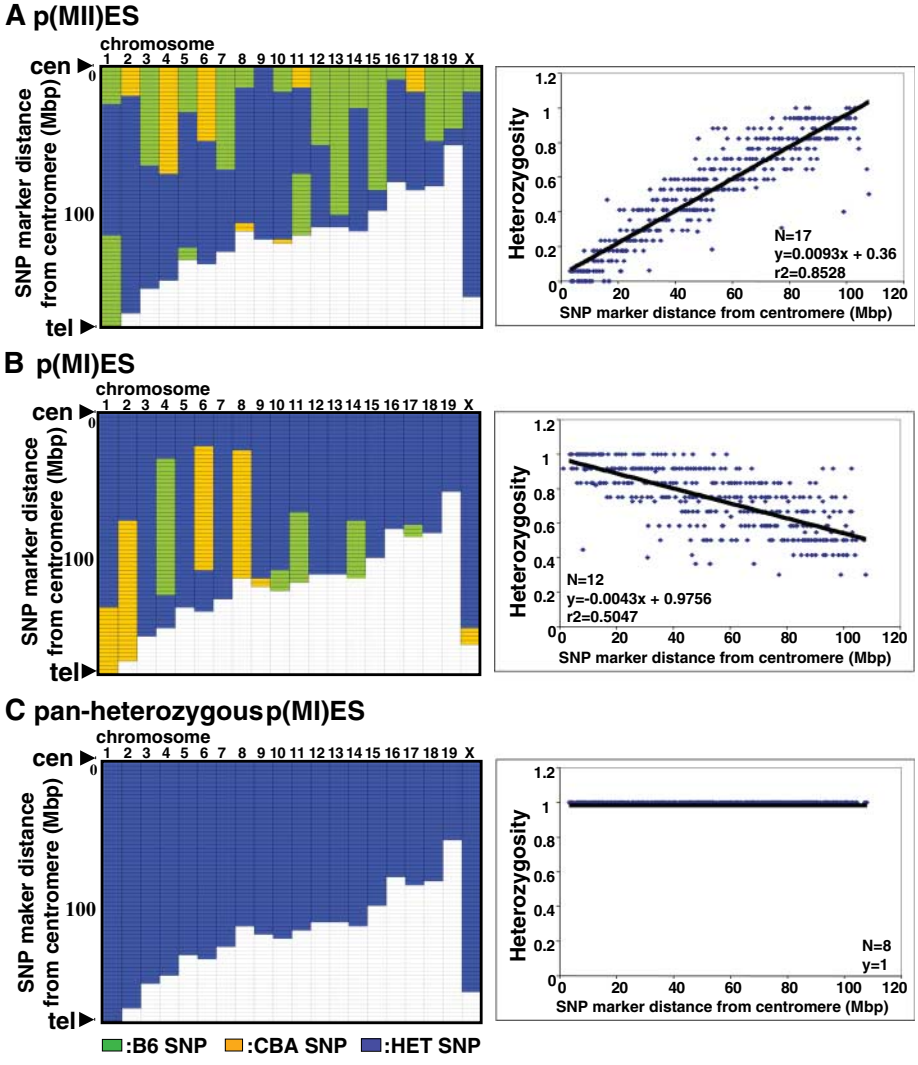

Fig. 3. Genome-wide SNP genotyping of a representative clone of p(MII)ES, p(MI)ES, and panheterozygous p(MI)ES cells. (**A**) p(MII)ES cells, (**B**) p(MI)ES cells, (**C**) panheterozygous p(MI)ES cells. Left panels show genotypes for each chromosome, from centromere (cen, top) to telomere (tel, bottom), revealing blocks, or haplotypes, of markers. Green, homozygous C57BL/6 (B6) SNP; orange, homozygous CBA SNP; blue, heterozygous (HET) SNP. Right panels show the heterozygosity of SNP markers plotted against SNP marker distance from the centromere.

Downloaded from www.sciencemag.org on May 13, 2010

after cytochalasin treatment to block MI, tetraploid blastocysts frequently result (figs. S2C and S9). Such embryos will yield tetraploid p(MI)ES cells, and it is possible that incubation with dimethylaminopurine may thereafter predispose them to abnormal chromosomal segregation or chromosomal loss. Such isolates maintain complete heterozygosity when genotyped as a population but do not represent a true clone of cells with genetic identity to the oocyte donor. Theoretically, parthenogenetic clones would arise only if the recombination events of MI are suppressed or if there is obligate co-segregation of the recombinant chromosomes into the same daughter cell. Based on our experience, we are skeptical that true parthenogenetic clones can be isolated.

Differentiation potential of p(MII)ES and p(MI)ES cell lines. To assess the pluripotency of the MHC-matched pES cells, we evaluated their differentiation potential by in vitro and in vivo assays. We injected cells subcutaneously into immunodeficient mice and observed robust teratoma formation from multiple p(MII)ES (n = 11), p(MI)ES (n = 4), and fES (n = 3) cell lines. The differentiation potential of p(MII)ES cells has been well documented (*1*), but not that of p(MI)ES cells. Histology of teratomas made from p(MI)ES cells revealed tissue elements of all three embryonic germ layers: mesoderm (bone, bone marrow, muscle, and cartilage), endoderm (respiratory epithelium and exocrine pancreas), and ectoderm [brain, melanocyte (iris), and skin] (Fig. 4). Using previously published methods for in vitro differentiation of ES cells, we observed rhythmic contractility in EBs that was consistent with cardiomyocyte development in pMI, pMII, and fES cells, and comparable numbers of hematopoietic elements as measured by methylcellulose-based colony-forming cell assays and flow cytometric analysis for the hematopoietic markers c-Kit, CD41, and CD45 (*20*) (fig. S10, A and B). We generated chimeric mice by injecting p(MII)ES (n = 4) and p(MI)ES (n = 3) cells into recipient blastocysts. Examples of p(MII)ES and p(MI)ES cells each demonstrated fetal liver chimerism and high-level skin chimerism of adult mice (Fig. 4I). No germline transmission of gametes from the p(MII)ES or p(MI)ES cells was noted in eight matings of female chimeras that generated more than 700 progeny. Moreover, injection of over 50 tetraploid embryos with p(MI)ES cells failed to result in live births, consistent with the known developmental limitation of parthenogenetic mouse embryos (*1*). Although not fully competent to sustain organismal development because of a lack of paternal imprints, p(MII)ES and p(MI)ES cells appear to share a comparable degree of multilineage tissue differentiation as fES cells.

Histocompatibility of differentiated progeny of MHC-matched p(MII) and p(MI)ES cells. To test the immune compatibility of selected ES cell lines, we performed transplantation experiments in immunodeficient mice and immunocompetent recipients that were either MHC-matched or -mismatched. When we injected 10^6 undifferentiated fES or pES cells subcutaneously into immunocompetent mice, we failed to observe efficient teratoma formation regardless of the genotypes of the ES cells or recipient mice. Like early embryonic tissues, undifferentiated mouse ES cells do not express MHC antigens, which we speculate renders them susceptible to rejection by NK cells (*5*). MHC antigens are expressed after differentiation of mouse ES cells in vitro (Fig. 2). To determine whether differentiated tissues derived from ES cells would be accepted as tissue grafts in recipient mice, we pre-differentiated ES cells into EBs for 2 weeks, then injected EB cells subcutaneously into immunodeficient mice or into immunocompetent MHC-matched and -mismatched recipients. We observed teratomas in all mice when we injected pre-differentiated ES cells into immunodeficient $Rag2^{-/-}/\gamma c^{-/-}$ mice (Table 2). In immunocompetent recipient mice, we observed teratoma formation from pre-differentiated fES and pES cells only if there was no MHC mismatch with the recipient (Table 2). All ES cells that carried both C57BL/6 and CBA MHC genotypes successfully engrafted in heterozygous MHC-matched C57BL/6 × CBA F_1 recipients, but failed to form teratomas in mismatched homozygous C57BL/6 or CBA recipi-

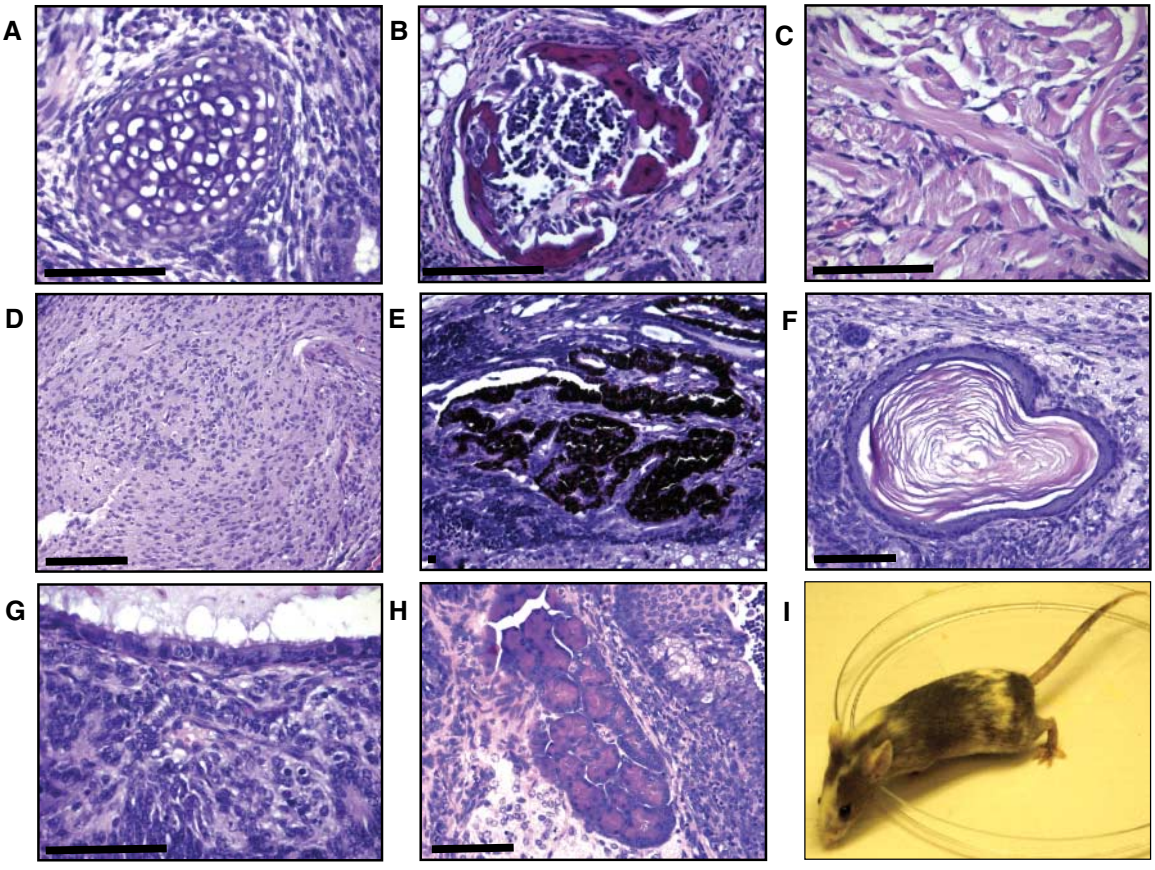

Fig. 4. Histopathology of teratomas from MHC-matched p(MI)ES cells and skin chimerism. (**A**) Cartilage. (**B**) Bone and bone marrow. (**C**) Muscle. (**D**) Brain. (**E**) Melanocyte (iris). (**F**) Skin. (**G**) Respiratory epithelium. (**H**) Pancreas. (**I**) Black coat color chimerism resulting from p(MI)ES cells injected into blastocysts from a BalbCSJL F_1 mouse (white coat color). Scale bar, 100 μm.

Downloaded from www.sciencemag.org on May 13, 2010

ents (Table 2). Homozygous fES or p(MII) ES cells engrafted in MHC-matched homozygous and heterozygous recipients (Table 2). Because ES cells of the CBA strain form teratomas in the $Rag2^{-/-}/\gamma c^{-/-}$ mice, which are on the C57BL/6 background, we conclude that the immune response, and not host strain factors, is responsible for the failure of teratoma formation in immunocompetent MHC-mismatched recipients. These data demonstrate the histocompatibility of differentiated tissues from fES and pES cells that share genetic identity at the MHC loci with transplant recipients.

Discussion. We describe two strategies for isolating pluripotent murine ES cells that are genetically matched to the oocyte donor at the MHC loci. By applying genotyping analysis to pES cells isolated from hybrid C57BL/6 × CBA F_1 mice, we have selected lines that retain the maternal MHC genotype by virtue of specific meiotic recombination events and inheritance of the relevant sister chromatids. When these genetically defined pES cells are pre-differentiated into EBs before being injected into immunocompetent recipient mice, the tissues engraft as long as the MHC genotype of the donor cells is matched to the recipient mouse.

Although unable to sustain full organismal development because of the lack of paternal imprints, ES cells derived from parthenogenetic embryos appear to be pluripotent. Whether tissue differentiation and engraftment into all lineages are robust and whether the loss of heterozygosity of critical genomic regions might disrupt cell function in engrafted tissues remain central questions (*21*). These caveats notwithstanding, our data from the murine system establish a proof of principle for using parthenogenesis to generate MHC-matched tissues for transplantation.

Differentiated tissues from pES cells that express only one of the two sets of parental MHC haplotypes appear to engraft in heterozygous recipients (for example, C57BL/6 into C57BL/6 × CBA F_1 recipients; Table 2). This suggests the theoretical possibility that a modest-sized bank consisting of pES cells homozygous for the major MHC haplotypes could serve as a source of transplantable tissues for cell replacement therapy. However, bone marrow and perhaps other tissues are subject to rejection by NK cells, which can distinguish tissues that express the full complement of MHC molecules from those expressing only a few (*10*). Moreover, minor histocompatibility antigens scattered across the genome might complicate transplantation from an allogeneic cell bank. Full MHC matching (or indeed, full genetic identity) is most favorable for predicting the survival and function of solid-organ allografts (*11*). More discriminating transplantation experiments are needed to distinguish the relative merits of tissues derived from homozygous MHC-matched pES cells, fully MHC-matched pES cells, or isogenic tissues derived by nuclear transfer.

A routine, highly efficient method for experimental parthenogenesis in mice interrupts MII and results in an embryo that carries a duplicated haploid genome that has been described as predominantly homozygous, except for regions that have reverted to heterozygosity because of recombination events during MI (*3*). Our data demonstrate quite unexpectedly that the majority of loci in p(MII)ES cells undergo recombination, thereby generating a predominantly heterozygous genome. Similarly, activation of immature oocytes and inhibition of the first meiotic division ensure that substantial heterozygosity is preserved across the genome, except for those regions that convert to homozygosity because of recombination. Both p(MII) and p(MI) cells can be selected to maintain the MHC genotype of the oocyte donor. All forms of pES cells retain the mitochondrial genome of the oocyte donor, unlike genetically matched ES cells that are created by nuclear transfer into oocytes from an unrelated donor, and therefore may avoid immunologic rejection due to antigens encoded by the mitochondrial genome (*22*).

Using a protocol that had been reported to create parthenogenetically cloned embryos (*16*), we generated a set of eight p(MI)ES cells that retained complete heterozygosity at all loci, implying genetic identity with the oocyte donor. However, these cells were all either tetraploid or aneuploid, suggesting that they arose from embryos that had failed to convert to diploidy during the parthenogenetic activation of immature oocytes. Although these cells retain essentially all of the maternal chromosomes, they are not true clones and are not likely to be a trustworthy source of tissues for transplantation.

The status of maternal- or paternal-specific imprint genes can be monitored to identify pES cells. Analysis of the imprinted status of the Rasgrf1 locus in 16 p(MI)ES cells confirmed the maternal pattern of methylation (fig. S11); however, the assessment of imprint loci in ES cells may be unreliable given their tendency toward epigenetic instability (*23*). The data presented here demonstrate that discerning the distinct patterns of homozygosity and heterozygosity in ES cell lines through SNP genotyping across the genome provides a definitive means to determine whether lines are the result of parthenogenesis, nuclear transfer, or natural fertilization. The diagnostic pattern of a p(MII)ES cell line is pericentromeric homozygosity and increasing heterozygosity as physical and genetic distance from the centromere increases. The diagnostic pattern of a p(MI)ES cell line is pericentromeric heterozygosity and an increasing frequency of homozygosity at markers distal to the centromere. A cell line derived from an embryo produced by nuclear transfer from a somatic cell will, for the most part, be a complete genetic match of the nuclear donor, because only rare occurrences of mitotic recombination would alter the expected pattern of SNP identity. Furthermore, there should be no discernable tendency for the recombination of genetic markers at greater distances from the centromere. Similarly, an ES cell line derived from a fertilized blastocyst should be a combination of sperm and egg donor haplotypes, again with no relationship between frequency of heterozygosity of markers and distance from the centromere.

Beyond demonstrating the potential for histocompatibility of parthenogenetically derived tissues, our experiments provide an analysis of genetic recombination during parthenogenetic activation and distinguish the patterns of recombination observed when karyokinesis is interrupted during meiosis I or II. Moreover, we note that isolation of p(MII)ES cells followed by SNP genotyping provides a means of genetic mapping of loci for phenotypes that can be defined through the study of ES cells.

References and Notes

1. N. D. Allen, S. C. Barton, K. Hilton, M. L. Norris, M. A. Surani, *Development* **120**, 1473 (1994).
2. J. B. Cibelli *et al.*, *Science* **295**, 819 (2002).
3. H. Lin *et al.*, *Stem Cells* **21**, 152 (2003).
4. L. Strain, J. P. Warner, T. Johnston, D. T. Bonthron, *Nat. Genet.* **11**, 164 (1995).
5. W. M. Rideout 3rd, K. Hochedlinger, M. Kyba, G. Q. Daley, R. Jaenisch, *Cell* **109**, 17 (2002).
6. H. Balakier, A. K. Tarkowski, *J. Embryol. Exp. Morphol.* **35**, 25 (1976).
7. E. J. Robertson, M. J. Evans, M. H. Kaufman, *J. Embryol. Exp. Morphol.* **74**, 297 (1983).
8. M. A. Surani, S. C. Barton, M. L. Norris, *Nature* **308**, 548 (1984).
9. C. J. Taylor *et al.*, *Lancet* **366**, 2019 (2005).
10. P. Hoglund *et al.*, *Immunol. Rev.* **155**, 11 (1997).
11. G. Opelz, T. Wujciak, B. Dohler, S. Scherer, J. Mytilineos, *Rev. Immunogenet.* **1**, 334 (1999).
12. National Center for Biotechnology information.
13. S. H. Klebs, M. W. Hoffmann, P. B. Musholt, B. Bayer, T. J. Musholt, *J. Immunol. Methods* **276**, 197 (2003).
14. E. Y. Fok, P. W. Zandstra, *Stem Cells* **23**, 1333 (2005).
15. I. Zvetkova *et al.*, *Nat. Genet.* **37**, 1274 (2005).
16. J. Kubiak, A. Paldi, M. Weber, B. Maro, *Development* **111**, 763 (1991).
17. The Jackson Laboratory, www.informatics.jax.org/ (2006).
18. J. L. Moran *et al.*, *Genome Res.* **16**, 436 (2006).
19. W. F. Dietrich *et al.*, *Nature* **380**, 149 (1996).
20. H. K. Mikkola, Y. Fujiwara, T. M. Schlaeger, D. Traver, S. H. Orkin, *Blood* **101**, 508 (2003).
21. L. Hernandez, S. Kozlov, G. Piras, C. L. Stewart, *Proc. Natl. Acad. Sci. U.S.A.* **100**, 13344 (2003).
22. J. Van de Water *et al.*, *N. Engl. J. Med.* **320**, 1377 (1989).
23. D. Humpherys *et al.*, *Science* **293**, 95 (2001).

24. This study was supported by grants from NIH and the NIH Director's Pioneer Award of the NIH Roadmap for Medical Research. G.Q.D. is a recipient of the Burroughs Wellcome Fund Clinical Scientist Award in Translational Research. K.K. was supported by the Cooley's Anemia Foundation and is a Special Scholar of the Leukemia and Lymphoma Society. P.L. was partly supported by NIH training grant Pathobiology of Newborn and Developmental Diseases (T32: HD07466). C.L. was supported by a Mildred Scheel Stiftung fuer Krebsforschung fellowship.

Supporting Online Material

www.sciencemag.org/cgi/content/full/1133542/DC1
Materials and Methods
Figs. S1 to S11
Table S1
References

7 August 2006; accepted 6 December 2006
Published online 14 December 2006;
10.1126/science.1133542
Include this information when citing this paper.

Downloaded from www.sciencemag.org on May 13, 2010

www.sciencemag.org/cgi/content/full/1133542/DC1

Supporting Online Material for

Histocompatible Embryonic Stem Cells by Parthenogenesis

Kitai Kim, Paul Lerou, Akiko Yabuuchi, Claudia Lengerke, Kitwa Ng, Jason West, Andrew Kirby, Mark J. Daly, George Q. Daley*

*To whom correspondence should be addressed. E-mail: george.daley@childrens.harvard.edu

Published 14 December 2006 on *Science* Express
DOI: 10.1126/science.1133542

This PDF file includes:

Supporting online material: Figures and Text

Supplementary Figure 1

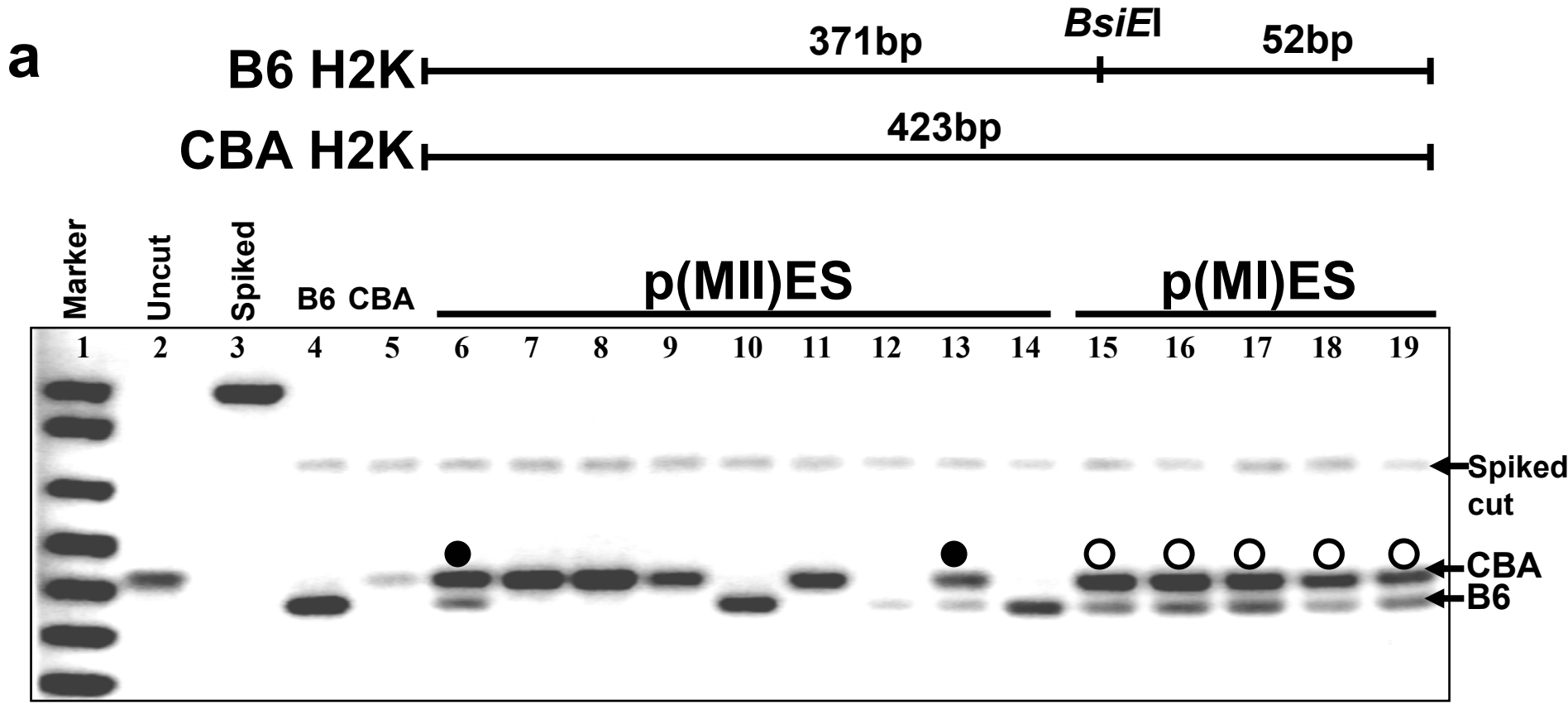

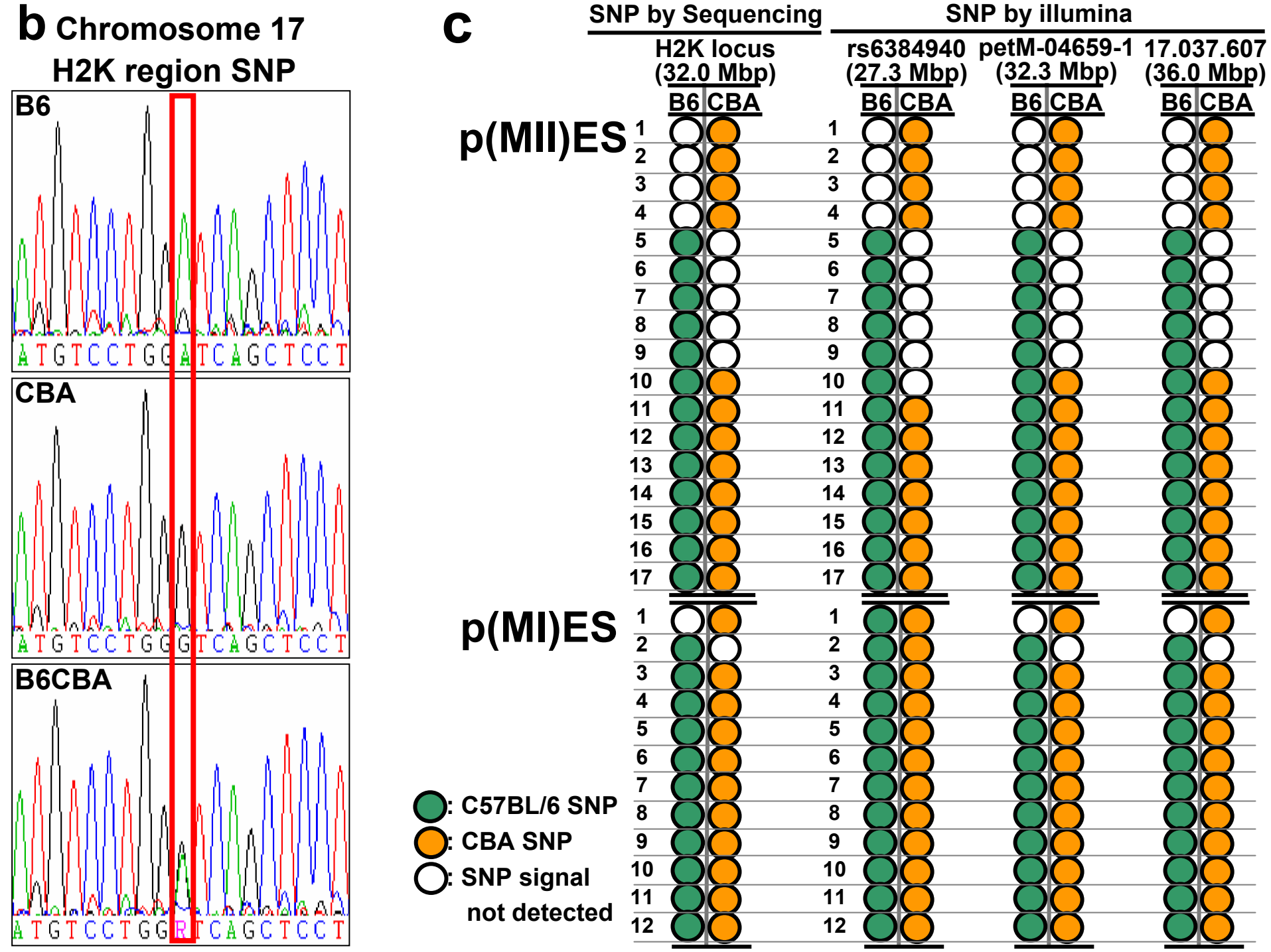
b Chromosome 17
H2K region SNP
B6
CBA
B6CBA
c
SNP by Sequencing
SNP by illumina
H2K locus (32.0 Mbp)
rs6384940 (27.3 Mbp)
petM-04659-1 (32.3 Mbp)
17.037.607 (36.0 Mbp)
B6 CBA
p(MII)ES
p(MI)ES
: C57BL/6 SNP
: CBA SNP
: SNP signal not detected

SOM Figure 1) Polymorphism studies on the Major Histocompatibility Complex (MHC) from C57BL/6 x CBA F1 pES cells. a, H2K gene. Schematic of PCR amplicon from H2K locus with C57BL/6 strain-specific *BsiE*I restriction enzyme site polymorphism (B6), and gel showing genotyping of genomic DNA samples by digestion of the PCR amplicon from the H2K region with the *BsiE*I restriction enzyme (*1*). Lane 1: 100bp size marker; lane 2: uncut PCR product; lane 3: uncut spiked DNA; lane 4: C57BL/6, digested with *BsiE*I; lane 5: CBA, incubated with *BsiE*I but not digested; lanes 6-14: nine p(MII)ES cells from B6CBAF1 mice incubated with *BsiE*I; lanes 15-19: five p(MI)ES cells from B6CBAF1 mice incubated with *BsiE*I. As internal controls for the completion of restriction enzyme digestion, samples 6-19 were spiked with a DNA fragment (arrow) containing a *BsiE*I restriction enzyme site. Black (closed) circles mark two p(MII)ES cells that have retained both haplotypes of the H2K genes. White (open) circles represent 5 p(MI)ES cells, each of which retain both haplotypes of the H2K genes. The amount of undigested (CBA) fragment exceeds the digested (B6) PCR fragment because of the inefficient restriction enzyme digestion of the heteroduplexes formed between the B6 and CBA alleles during PCR amplification. **b,** Representative sequencing results to demonstrate detection of different SNP signals for homozygous C57BL/6 and CBA, as well as heterozygous B6CBAF1 for H2K MHC region SNP on chromosome 17. **c,** Results of SNP genotyping of markers within or flanking the H2K MHC region of chromosome 17 in 17 p(MII) and 12 p(MI) ES cell lines either by DNA sequencing or by the Illumina multiplexed allele extension and ligation method. Mbp units under locus marker indicate the physical map distance from the centromere. Marker rs6384940 is immediately proximal to H2K; marker petM-04659-1 is within H2K locus; marker 17.037.607 is immediately distal to H2K.

Supplementary Figure 2

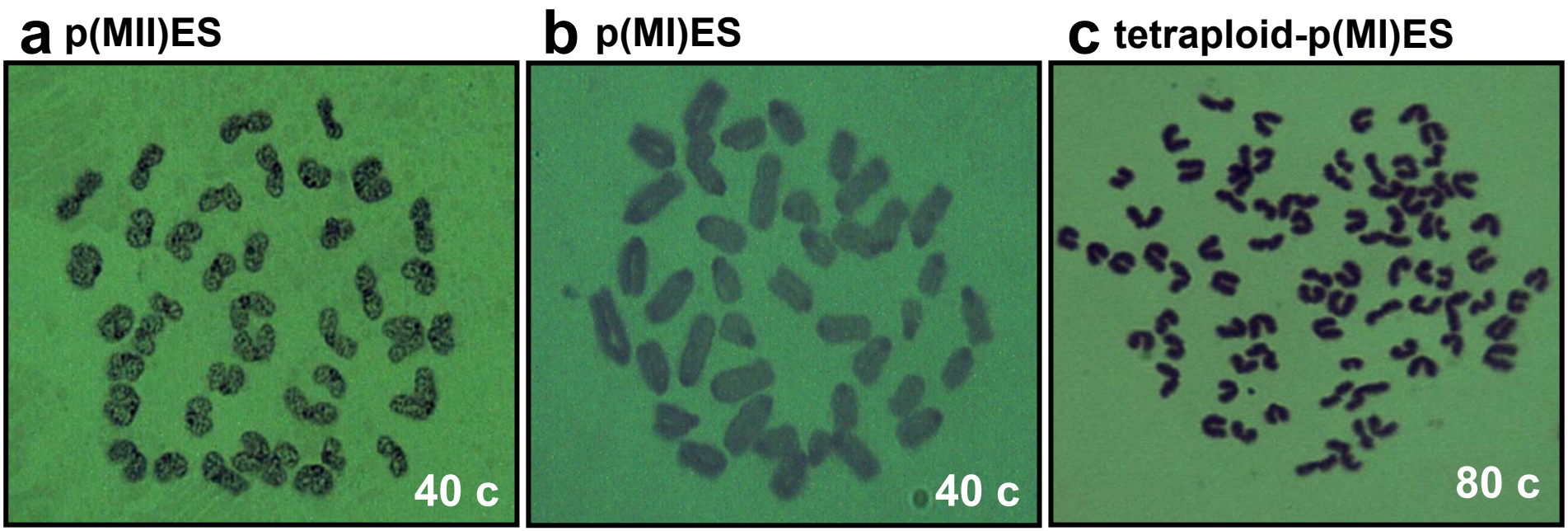

SOM Figure 2) Metaphase preparations of chromosomes of representative p(MII)ES, p(MI)ES, and tetraploid-p(MI)ES cells.

Supplementary Figure 3

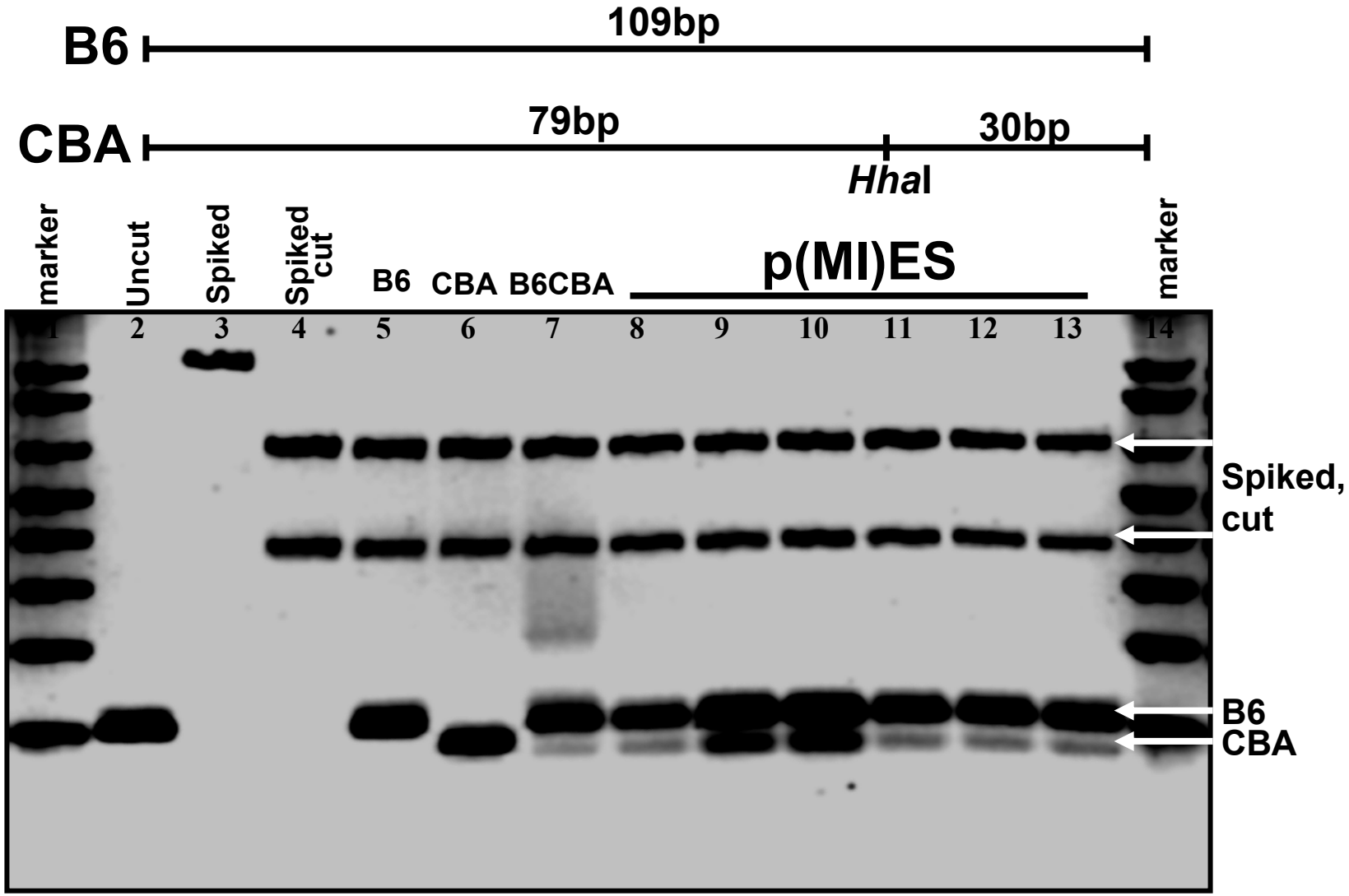

SOM Figure 3) Polymorphism studies on the Tap1 gene in C57BL/6 x CBA F1 MHC-matched p(MI)ES cell lines. Schematic of PCR amplified region of Tap1 gene on chromosome 17. *Hha*I restriction enzyme site is absent in C57BL/6, but present in CBA strain. **Genotyping by *Hha*I digestion of Tap1 gene PCR amplicon.** The Tap1 gene is only 0.05cM away from H2K gene, but whereas the H2K allele PCR product is digested by *BsiE*I in C57BL/6 but not in CBA, the Tap1 gene PCR product is digested by *Hha*I in CBA but not in C57BL/6. Using this reverse pattern of PCR product digestion, we demonstrated that all MHC-matched p(MI)ES lines were heterozygous for the polymorphism at the Tap1 locus – a gene neighboring the MHC locus. Lane 1: 100bp size marker; lane 2: uncut PCR product; lane 3: uncut spiked DNA; lane 4: spiked DNA, *Hha*I digested; lane 5: C57BL/6 incubated with *Hha*I but not digested; lane 6: CBA *Hha*I digested; lane 7: B6CBAF1 incubated with *Hha*I, note that both fragments are present; lane 8-13: seven MHC-matched p(MI)ES cells from B6CBAF1 mice incubated with *Hha*I and showing both fragments, confirming heterozyogisity at this locus; lane 14: 100bp size marker. As internal controls for complete restriction enzyme digestion, samples 5-13 were spiked with a DNA fragment containing *Hha*I restriction enzyme sites (see lanes 3 and 4).

Supplementary Figure 4

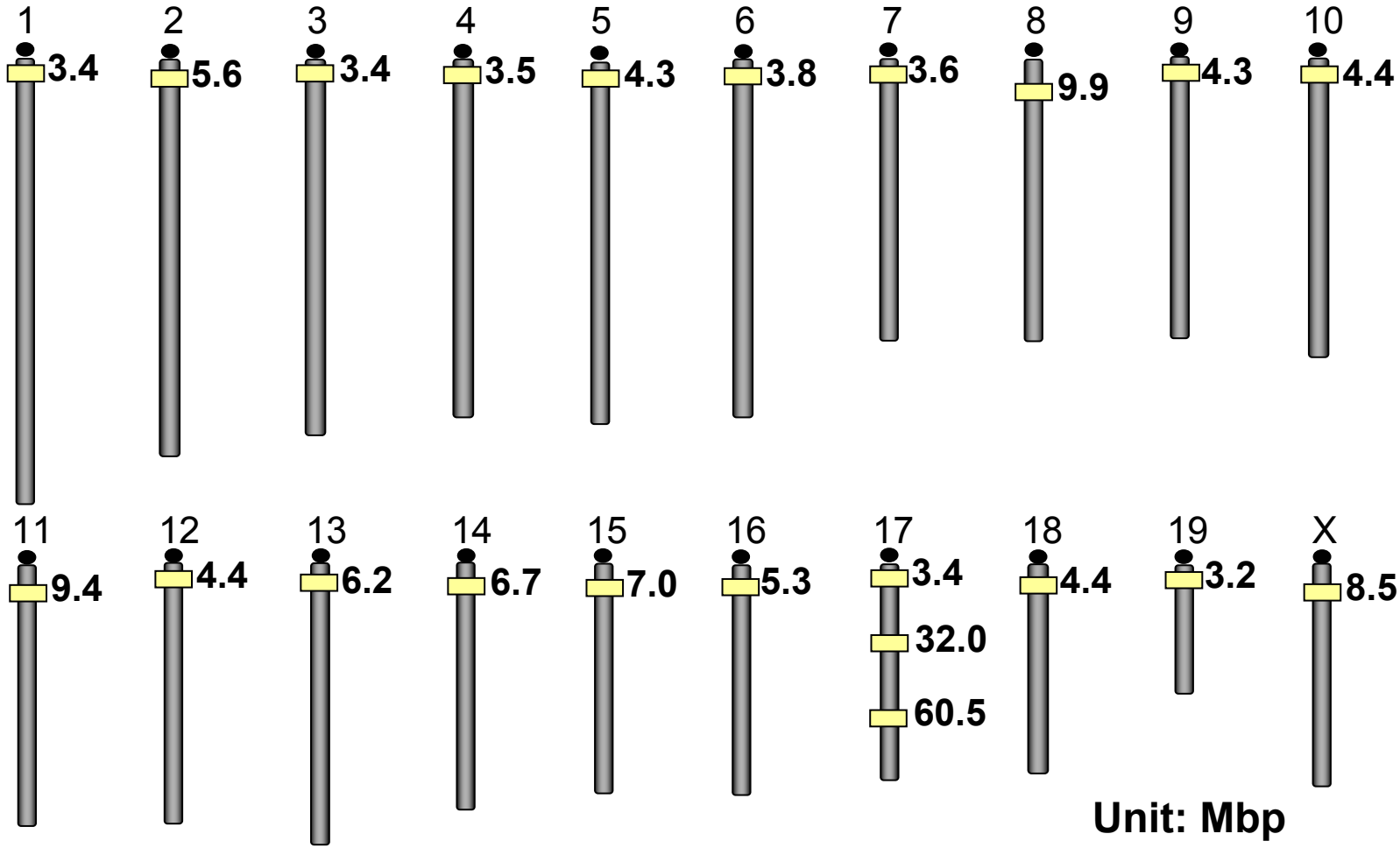

Pericentromeric genotype in p(MII) and p(MI)ES cells. To analyze the pattern of chromosomal segregation induced under the different oocyte activation protocols, we sought to determine the peri-centromeric genotype and the patterns of recombination of the p(MII)ES and p(MI)ES cell lines using SNPs that distinguish the parental mouse strains (C57BL/6 and CBA) (*2*). We selected an informative SNP locus on each chromosome close to the centromere that should sustain minimal recombination (average distance, 5.5 Mbp; Fig. S4). The locus harboring the SNP was amplified by PCR and sequenced, which allowed us to distinguish C57BL/6, CBA, and B6CBAF1 specific profiles (not shown). As hypothesized, p(MII)ES cells were found to be homozygous for either the C57BL/6 or CBA peri-centromeric SNPs (Fig. S5c), whereas all but one of 5 p(MI)ES cells were found to be heterozygous for all peri-centromeric SNPs tested (Fig. S5d-h). Homozygosity of one locus in one p(MI)ES cell (Fig. S5h) suggested either chromosome loss or recombination.

SOM Figure 4) Location of peri-centromeric SNP markers on all chromosomes and distal markers on chromosome 17

Supplementary Figure 5

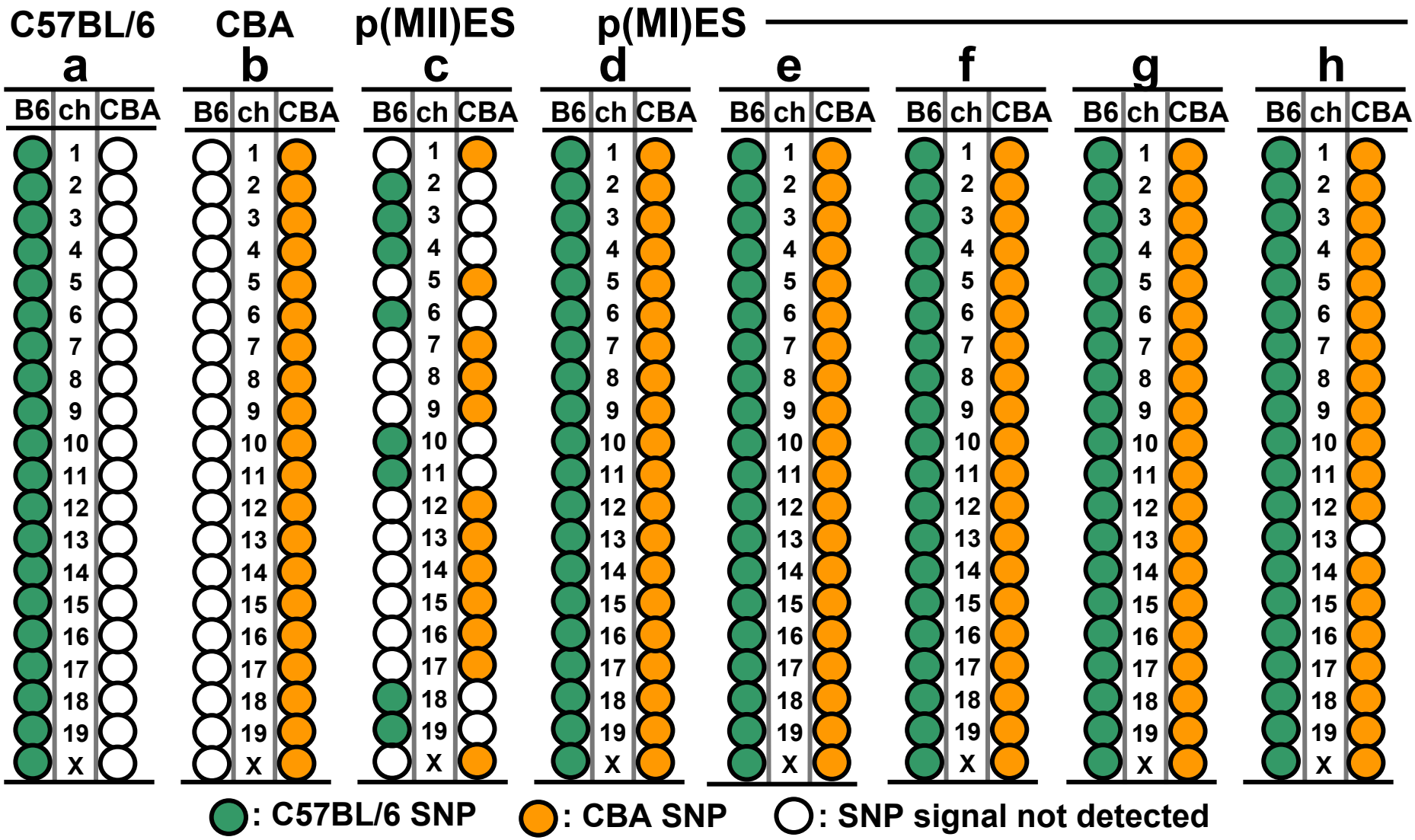

SOM Figure 5) Genotyping of peri-centromeric SNPs in p(MII)ES and p(MI)ES cells to determine homozygosity or heterozygosity. Strain specific SNP signals for C57BL/6, CBA, or B6CBAF1 were detected by sequencing of a PCR amplicon that harbored a strain-specific SNP. Loci for which the SNP allele was detected are marked in color beneath the relevant strain. Chromosome number of the SNP is indicated. Genomic DNA samples from C57BL/6 and CBA mice were tested as controls (a, b). Genomic DNA from one p(MII)ES cell line (c) and five p(MI)ES cell lines (d-h) were tested at SNPs located within 3.4-9.9 Mbps of the centromere.

Supplementary Figure 6

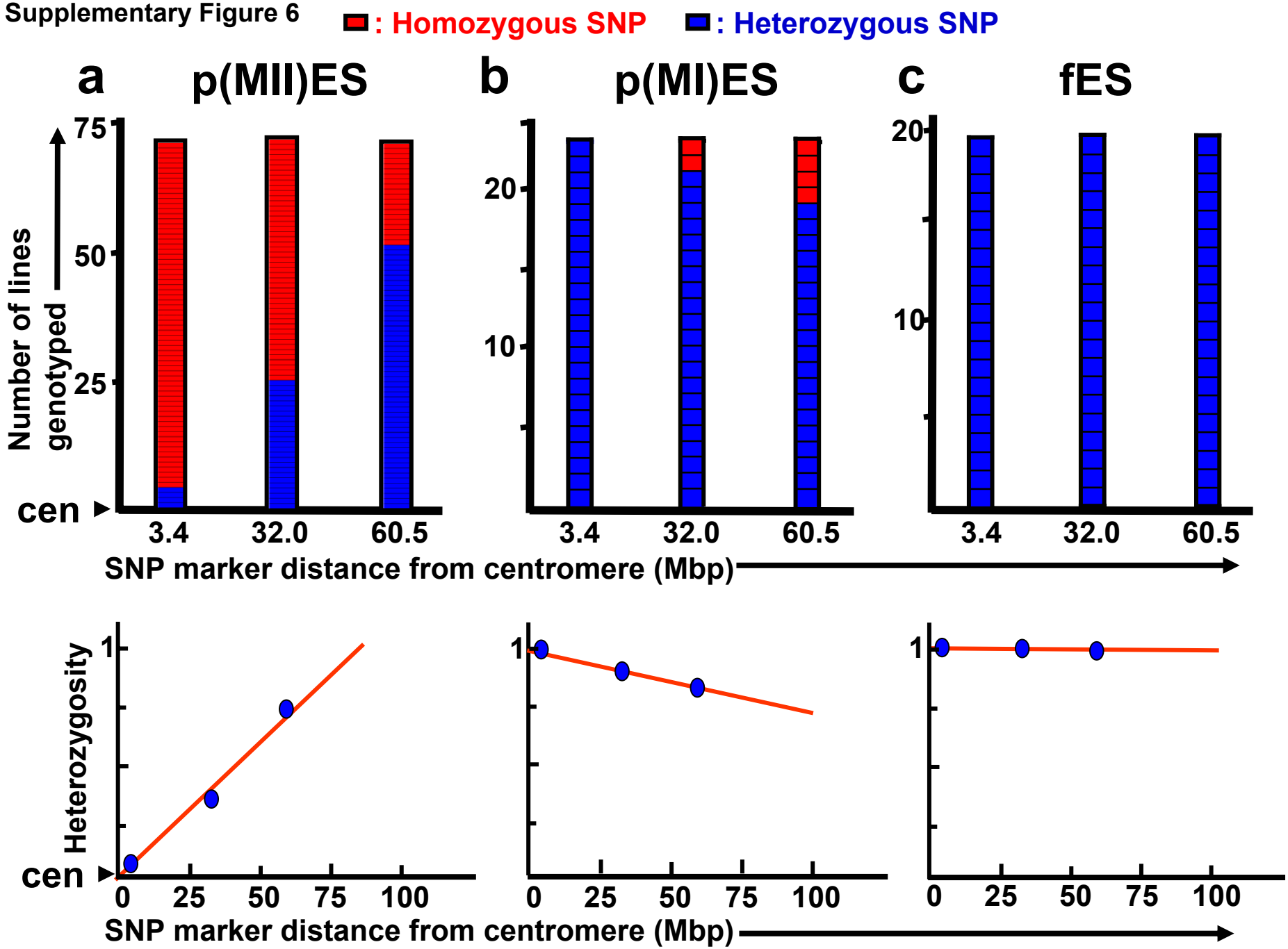

Recombination patterns of the p(MII) and p(MI)ES cells. To analyze the frequency and distribution of recombination events in p(MII)ES and p(MI)ES cells, we performed additional SNP genotyping at 3 loci located at 3.4Mbp (4.0 cM), 32.0Mbp (18.65 cM), and 60.5Mbp (33.5 cM) from the centromere of chromosome 17 (Fig. S4). Given the nature of the two distinct protocols for parthenogenetic activation, we reasoned that p(MII)ES cells would have predominant peri-centromeric homozygosity, with recombination reflected by a telomeric predominance of heterozygous SNPs. A survey of 72 independent clones of p(MII)ES cells indeed confirmed that the frequency of heterozygous SNPs increased in proportion to the distance from the centromere to the SNP (Fig. S6a). Conversely, we reasoned that the p(MI)ES cells would have predominant peri-centromeric heterozygosity, with recombination reflected by a telomeric predominance of homozygous SNPs. In a survey of 23 p(MI)ES cell lines, the frequency of homozygous SNPs increased in proportion to the distance from the centromere to the genetic markers (Fig. S6b). ES cells isolated from embryos that result from natural fertilization events between strains of inbred mice (fES cells from F1 matings) should show heterozygosity at all loci, because the gametes derive from homozygous parents in which meiotic recombination is genetically invisible. As anticipated, we detected complete heterozygosity at the three SNP loci on chromosome 17 in 20 fES cell lines (Fig. S6c). Therefore, by plotting the heterozygosity rate *vs*. marker distance from the centromere, we can readily determine whether an ES cell represents the p(MI)ES, p(MII)ES, or fES type (Fig. S6, lower panels).

SOM Figure 6) Recombination in p(MII)ES, p(MI)ES, and fES cells detected by genotyping of chromosome 17 SNPs. Upper panels: ES cell lines were examined for C57BL/6 and CBA strain-specific SNP signals at 3.4Mbp, 32.0Mbp, and 60.5Mbp from the centromere on chromosome 17. Blue indicates a heterozygous genotype; red indicates homozygous. **a,** p(MII)ES; **b,** p(MI)ES; **c,** fES cells. **Bottom panels:** The heterozygosity at each locus, calculated as frequency of heterozygosity/ total number of cell lines genotyped, was plotted against the SNP marker distance from the centromere of chromosome 17.

Supplementary Figure 7

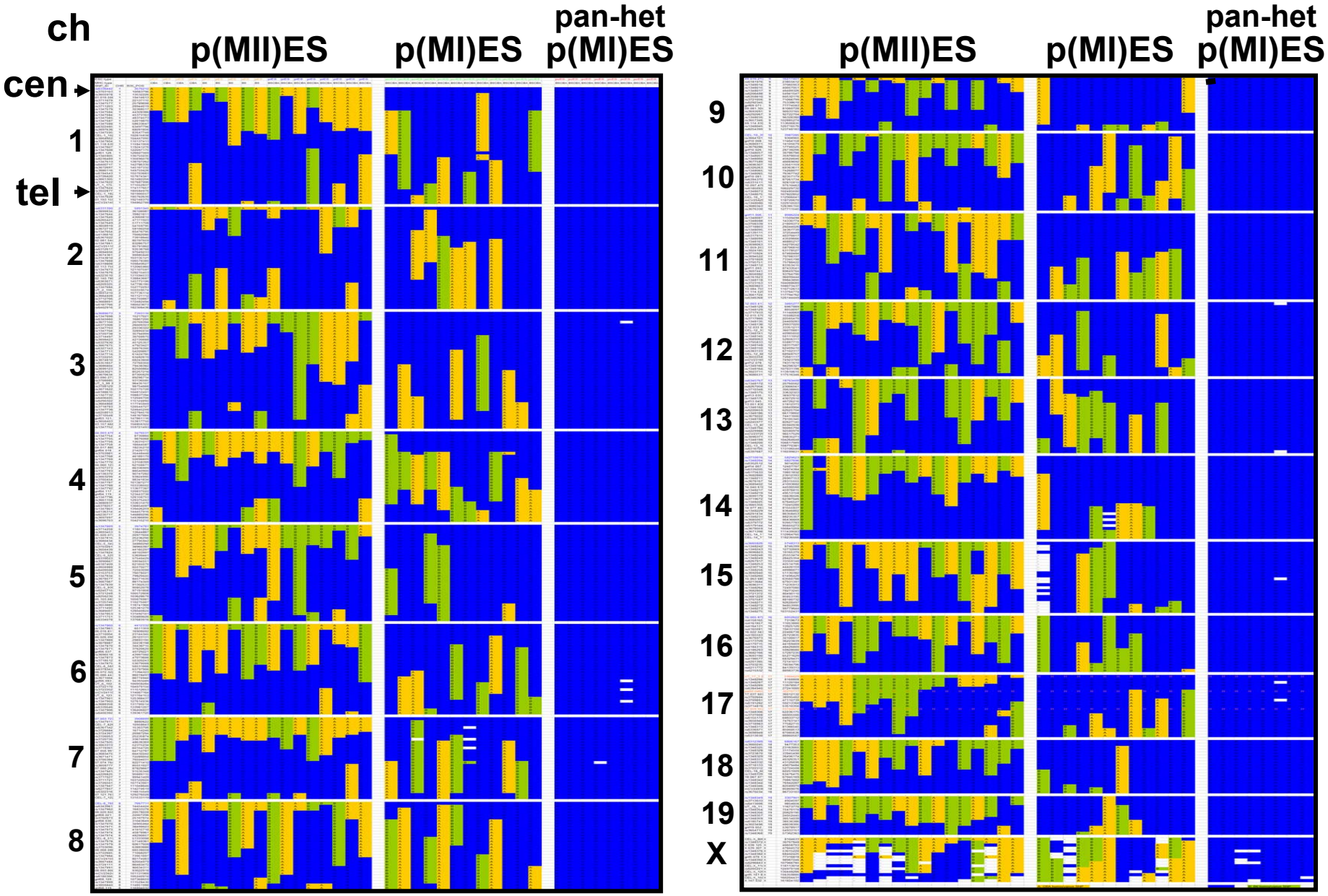

SOM Figure 7) SNP genotype data. The raw SNP genotype data have been organized into groups: p(MII)ES cells; p(MI)ES cells; and pan-heterozygous ES cells. All informative SNP markers are ordered from top to bottom, centromere ("cen") to telomere ("tel") for all chromosomes (1-19, X), and colored to indicate homozygous C57BL/6 (green color), homozygous CBA (orange color), or heterozygous B6CBA (blue color) genotypes in native chromosome locations. Note that p(MII)ES cells show peri-centromeric homozygosity and blocks of recombined heterozygous markers more distally on each chromosome; p(MI)ES cells show peri-centromeric heterozygosity and blocks of homozygous markers more distally; pan-heterozygous p(MI)ES cells show an apparent lack of any recombination, although we speculate that all recombined chromosomes have been retained in the cell (subject to random loss in sub-clones of the population, leading to population aneuploidy but preserving pan-heterozygosity of all genotypes).

Supplementary Figure 8

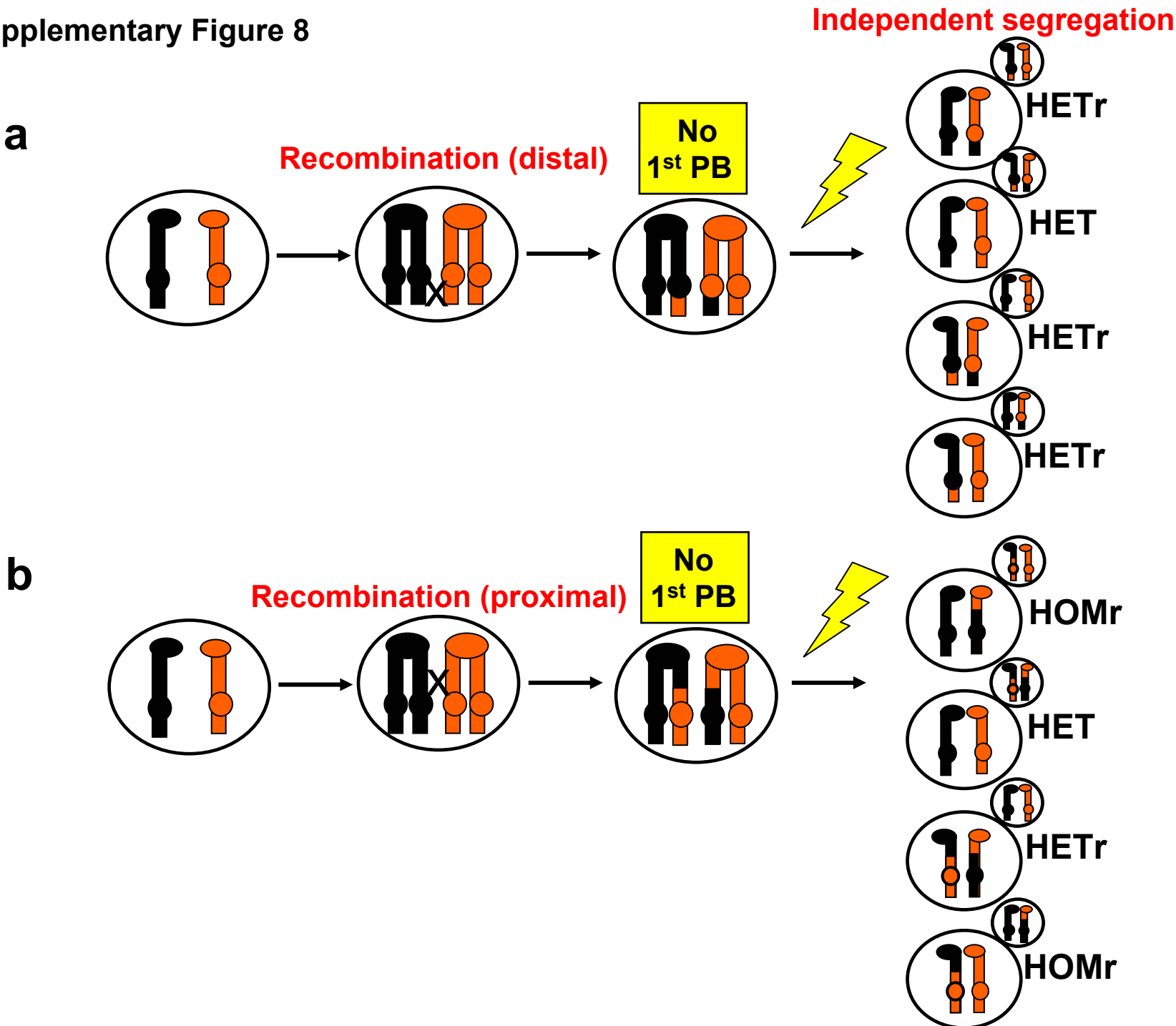

SOM Figure 8) Allelic segregation during MI parthenogenesis. The genotyping data on the p(MI)ES cells demonstrates significant suppression of the genome map (910cM). One model to explain this apparent suppression of recombination is co-segregation of recombinant chromatids in the second meiotic division (in apparent violation of Sturtevant's rule, which dictates that recombinant chromosomes segregate independently). A schema is shown that demonstrates the possible outcomes of the chromatid segregation process, assuming independent segregation after recombination events on one homologous chromatid pair (obligate co-segregation due to non-disjunction is an alternative model). **a,** If crossing over has not occurred at the MHC region (distal recombination), all 4 genotypes will remain heterozygous at the MHC locus. **b,** If crossing over has occurred proximal to the MHC region and chromatids that exchanged DNA during crossing over do not segregate together, homozygosity at the locus will be generated (HOMr). Alternatively, if the chromatids that exchanged DNA during crossing over at the MHC do segregate together (either by chance or non-disjunction), heterozygosity at the locus will be restored (HET/HETr). For simplicity, recombination involving only one of the two sister chromatids is shown. In fact, both sisters of paired homologues may undergo recombination, which will yield a more complex pattern of genotypes, but all tending to favor maintenance of heterozygosity. Different parental origins of homologous chromosomes are represented by distinct colors. The MHC locus is represented by circles.

Supplementary Figure 9

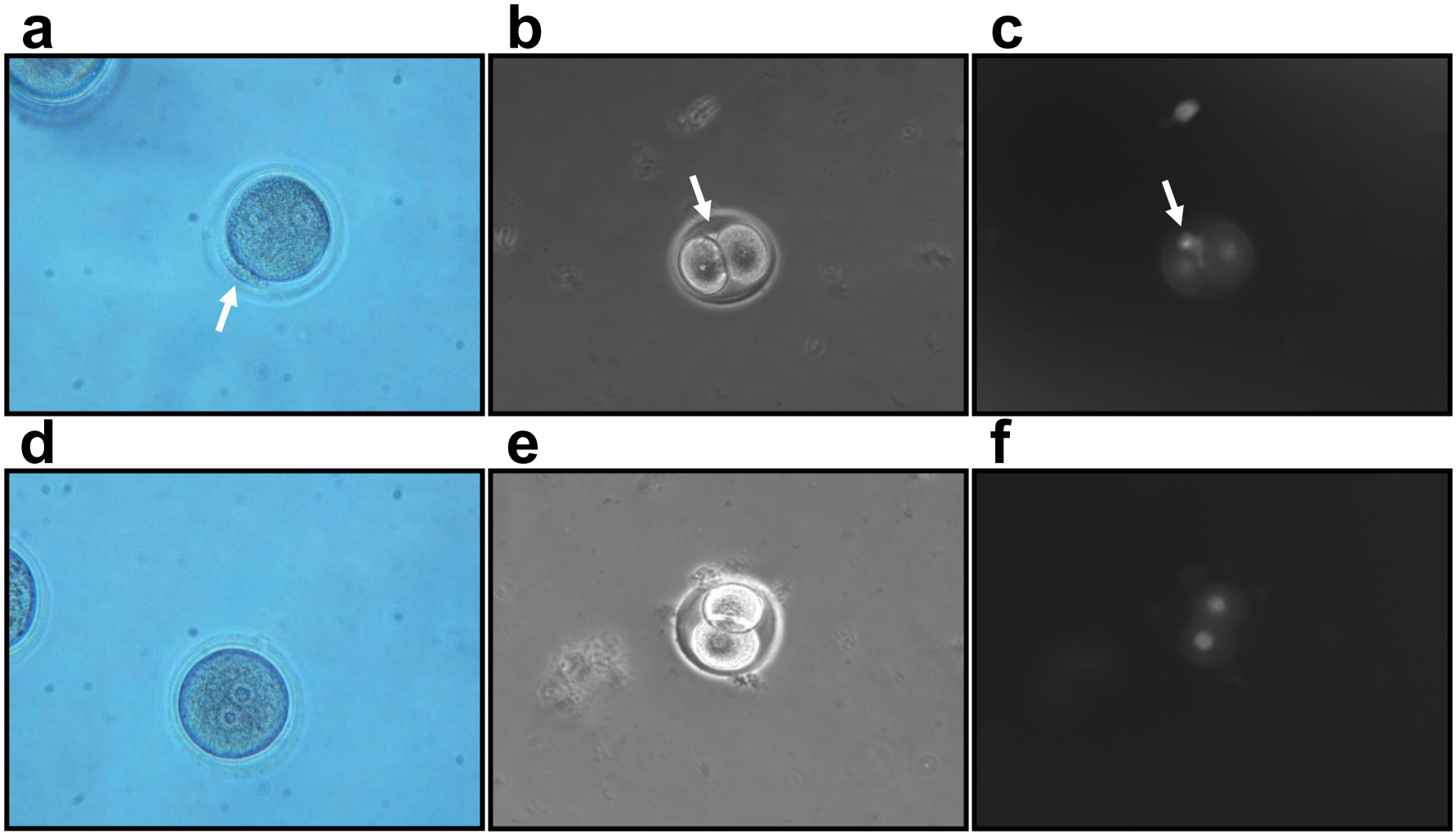

SOM Figure 9) Development of embryos that yield diploid p(MI)ES and tetraploid p(MI)ES cells. a, An immature oocyte activated 6 hours after cytochalasin D treatment resulted in an embryo with two pronuclei and a polar body. **b,** the embryo in a, shown at the 2-cell stage. Note that the polar body remains visible (arrow). **c,** Hoechst 33342 staining of the 2-cell stage embryo demonstrates genetic material in the polar body (arrow). Embryos of this type produced diploid p(MI)ES cells. **d,** An immature oocyte activated spontaneously or in 1 hour after cytochalasin D treatment. Due to residual cytochalasin D, the polar body extrusion was inhibited, and two pronuclei are visible. The embryo subsequently cleaved normally to the 2-cell stage. **f,** Hoechst 33342 staining of the 2-cell stage embryo shows no genetic material in the perivitelline space, where the polar body would be located. The ES cells isolated from embryos of this class contained 80 chromosomes (Fig. S1c).

Supplementary Figure 10

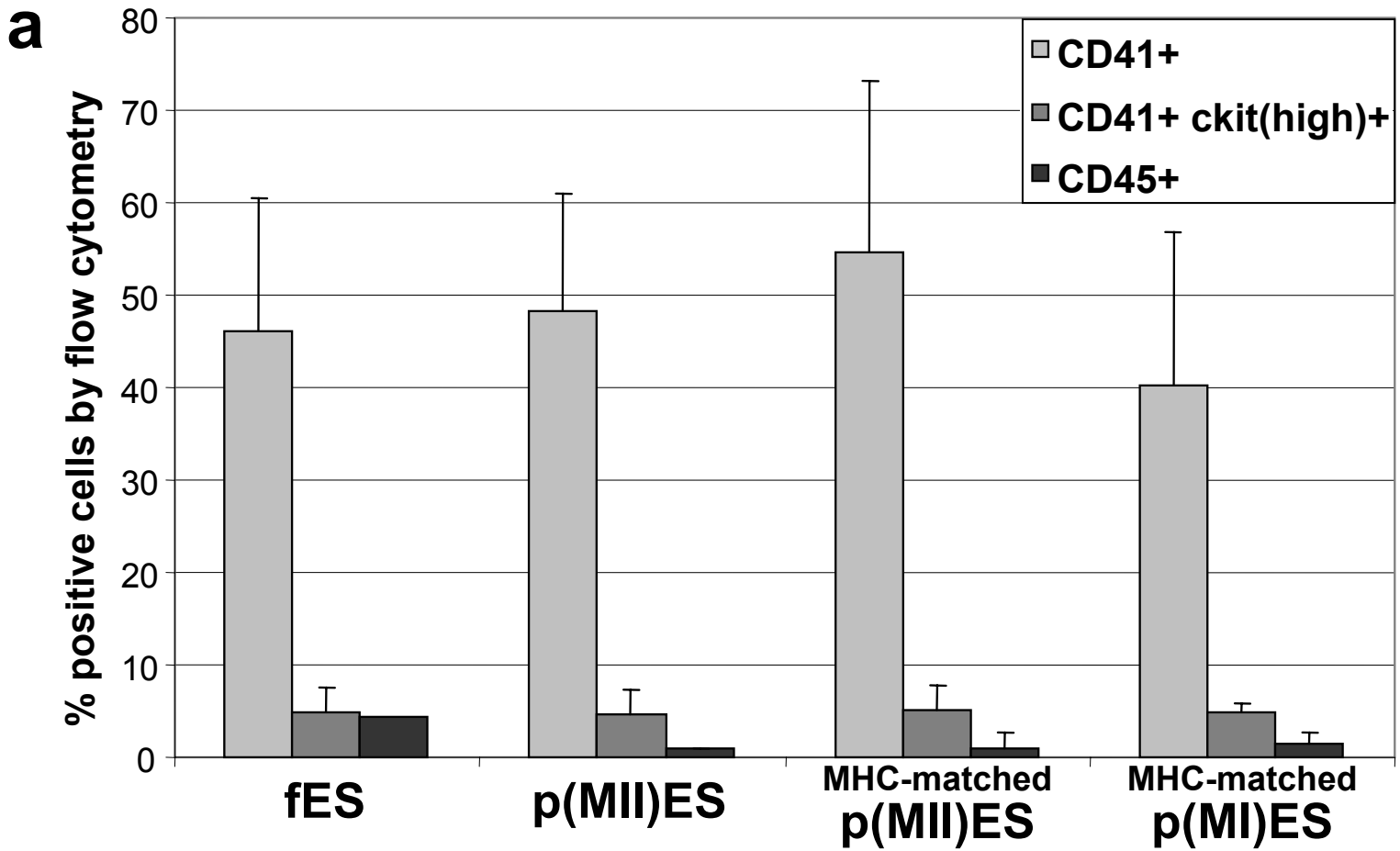

Supplementary Figure 10

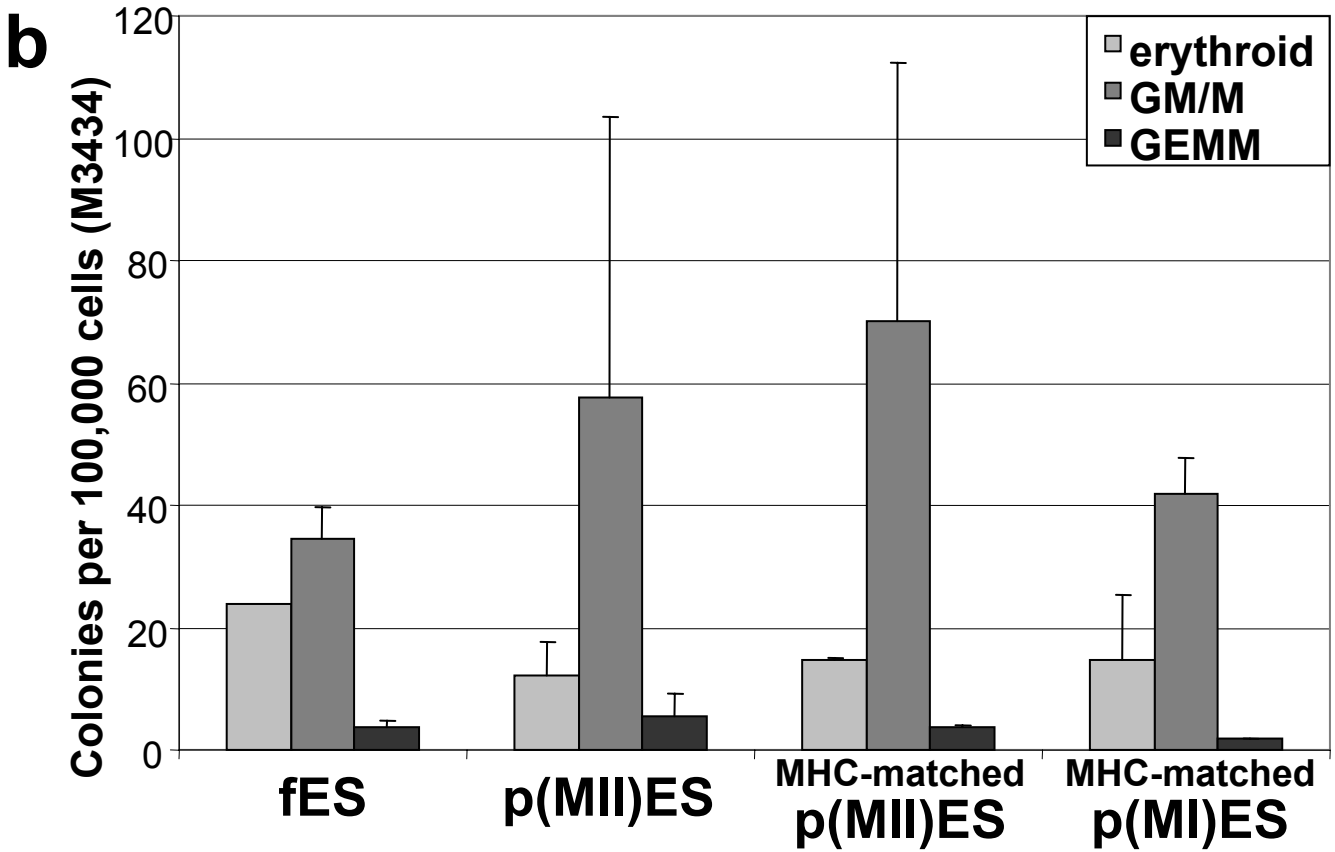

SOM Figure 10) Hematopoietic developmental potential of p(MII)ES, MHC-matched p(MII)ES, and MHC-matched p(MI)ES cells. a, Flow cytometry on day 6 EB-derived cells. p(MII)ES, MHC-matched p(MII)ES (N=2), MHC-matched p(MI)ES (N=2), or fES cells were stained with relevant antibodies to detect CD41+, CD41+ ckit-high+, and CD45+ hematopoietic cells. All ES cells showed equivalent hematopoietic populations. **b,** Formation of myeloid colonies in methylcellulose supplemented with hematopoietic cytokines (M3434; Stem Cell Technologies). Colony numbers are per 100,000 cells from day 6 EBs. Robust hematopoietic colonies, displaying a similar hematopoietic lineage contribution can be observed in all ES cell lines.

Supplementary Figure 11

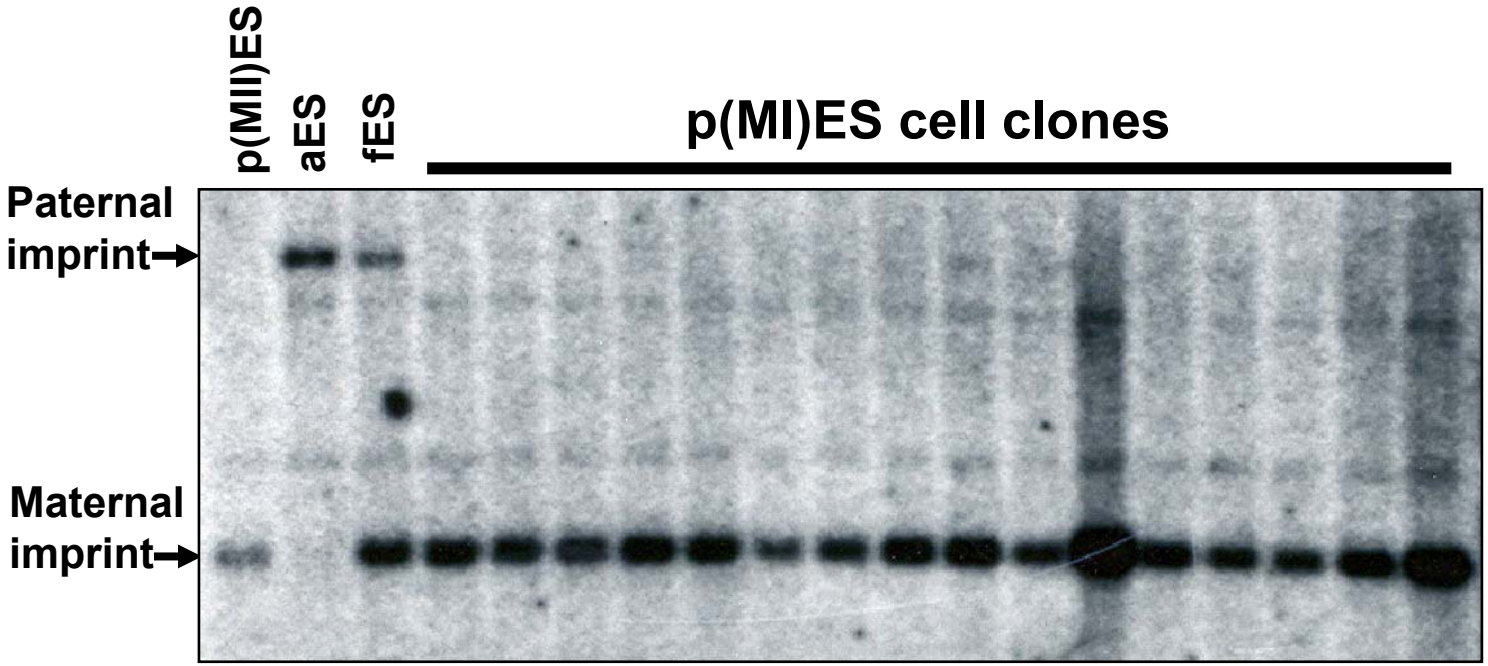

SOM Figure 11) Southern blot analysis to determine the methylation status of the imprinted Rasgrf1 locus in p(MI)ES cells. During germ cell development, the unique parental methylation marks, or imprints, are first erased in the primordial germ cells and later re-established during oogenesis or spermiogenesis so that specific loci are expressed from either the maternally or paternally inherited allele. Because p(MI)ES cells are established after the re-establishment of imprints in the growing oocyte (*3*), they should lack paternal imprints and carry only maternal methylation marks on both chromosomes. We used the methylation sensitive restriction endonucleases *Pst*I/*Not*I to digest genomic DNA isolated from p(MII)ES, p(MI)ES, and androgenetic ES cells (aES, derived from blastocysts developed from two sperm pronuclei) (*4*) to distinguish the allele that carries paternal *vs.* maternal methylation marks. Genomic DNA of 16 p(MI)ES cell clones and controls were digested with *Pst*I/*Not*I, and hybridized with a probe from the Rasgrf1 gene, as described (*5*). This locus is typically methylated on the paternal allele, which renders it resistant to restriction digestion, thereby yielding a fragment length of 8 kbp. The unmethylated maternal allele results in a 3 kbp fragment. Digestion of parthenogenetic ES cells (p(MII)ES) shows the maternal allele. Digestion of androgenetic ES cells (aES) that are derived from reconstruction of a zygote with 2 male pronuclei shows only the paternal alleles, while ES cells isolated from fertilized embryos (fES) shows both. All p(MI)ES cell clones reveal the maternal pattern, consistent with their derivation from cells that harbor only a maternal genome.

Supporting Online Table SI Primers used in this study (Chromosome number: distance from centromere (bp)).

SNP PCR amplication primer set		SNP PCR sequencing primer
Chr1:3354789	Chr12:4427782	Chr 1: 5'- CAC TGG AAG GAG GAA TTT CA -3'
5'- TGT TCC AGG TCA GTG ACT TCC -3'	5'- AAC TGG CCT AAG GGT CCA CT -3'	Chr 2: 5'- CCT TTC ATG AAG CAG ATG ACA -3'
5'- GCC TTT TTC AAC TTG CCT CA -3'	5'- CTG AGA CAT TGT CCC GCT TT -3'	Chr 3: 5'- GCT GCT ACA AAT ACT AAG AAA TGT TCC -3'
Chr2:5609234	Chr13:6192628	Chr 4: 5'- GCT TTT GAT TTG TTG TCT TTT TGA -3'
5'- CAA CAG AAA GGA GGC CAA AG -3'	5'- TGT CTT CGC ACA TCT TGT CC -3'	Chr 5: 5'- CAG TTG GAA TGT CCA TCA GC -3'
5'- TCA GTA CCA AGC ACG TGA GC -3'	5'- TAA GCC AGC TTC TTC CAA GC -3'	Chr 6: 5'- TCA GCT AAA GCA TAT TAA TTC AAA ACA -3'
Chr3:3750240	Chr14:6685859	Chr 7: 5'- TAG GTG GGC ATG GGT GAG TA -3'
5'- TGC TTA TGG TTT TAT GTA ATA GGC -3'	5'- GCT CCA GAA CCA AGA ACT GC -3'	Chr 8: 5'- CCG AGC AGC TGG TAT TTG AT -3'
5'- TTT ATG CCA TGG TCC TTT GG -3'	5'- AAA CAG CCT GAT CCC AAT GT -3'	Chr 9: 5'- TGA TAA ATG AGA CCA CGA TAC CA -3'
Chr4:3476531	Chr15:6955482	Chr10: 5'- CAG TGA AGA GCA CAC CCA TT -3'
5'- AAA CAT GGA GCT CTC TGA AAA TG -3'	5'- AGA GTG GCC CAG AAA GTT CA -3'	Chr11: 5'- GGC ATT GGC TAG ATA CAC AAA A -3'
5'- AGG AGG TGC AAT TCA GCT TT -3'	5'- CCA GCT CCA CTC CTA ACA GC -3'	Chr12: 5'- TCA TTC TTT GCT GTG GAA ACA -3'
Chr5:4310159	Chr16:5321310	Chr13: 5'- CCC CAA AAG TAG ACA ATT TCC TT -3'
5'- GCA ATT GCT GTT GAA AGC TG -3'	5'- TGG CAC ACT TGT GAC AAC CT -3'	Chr14: 5'- TGG TTT GAT CAA TAG TTT CTT AGG G -3'
5'- AAT GCC AAA CCC ATC CAT TA -3'	5'- GAT CTG ATG CTT CCC TGG AT -3'	Chr15: 5'- CCC AAG AGA GGA GGG AGT TT -3'
Chr6:3799842	Chr17:3383258	Chr16: 5'- ATC TCT GAT CCC AGG AGG TG -3'
5'- TGG TCC AAA TTT CCA TCA GC -3'	5'- CCC CTC CGA CAG AAC ATC TA -3'	Chr17: 5'- TGA GAA TTT CAT GCG AGA GC -3'
5'- TGC CAG GCA TAT GGT TAG TG -3'	5'- GGT GAC AAG GGG TTT GAA GA -3'	Chr17: 32 Mbp region (H2-K)
Chr7:3581601	Chr17: 32 Mbp region (H2-K)	5'- CCT GGG CTT CTA CCC TGC T -3' or
5'- ATG GTT TGG GGG TAG AGG TC -3'	5'- CCT GGG CTT CTA CCC TGC T -3'	5'- CCA CCA CAG CTC CAG TGA G -3'
5'- CCA CAA TAC TGA AGG GCA CA -3'	5'- CCA CCA CAG CTC CAG TGA G -3'	Chr17: 5'- CTC ACA AAA CCT GCC CTT GT -3'
Chr8:9889063	Ch17: 60455318	Chr18: 5'- GTG GGT AGC TCT GCT GAA GG -3'
5'- CCA CCA GCC TTT CCT AAA CA -3'	5'- TGC TTA CCC TCA GCA AGA CA -3'	Chr19: 5'- AAG GAG CAG GAA CTC ATC ACA -3'
5'- CCT CAA CCC AGA TCT CTC CA -3'	5'- TTC TGG GTA GCT CAG GCT GT -3'	Chr X: 5'- AAG GAG CAG GAA CTC ATC ACA -3'
Chr9:4289768	Chr18:4445867	
5'- GGT CTC AAG CAG GTG AGC TT -3'	5'- CAC AGA TGT CAG CTC CGT GA -3'	
5'- TTC TCA AAA TCT TTT TGG ATG C -3'	5'- TTC CAA CTC CTC CAC TCA GG -3'	
Chr10:4381768	Chr19:3243816	
5'- GAG GGA CTC ACA AGC CAC AT -3'	5'- TCA TTC GGC CAA TAC ACA GA -3'	
5'- CCT TCT GGC CTT CTG TGA AC -3'	5'- GGG AAA GGA CTT AGG CTT GC -3'	
Chr11:9447523	ChrX:8450263	
5'- CTC ATT TGG AGG CCT CTG TC -3'	5'- AAA TCA ACT CTT GCG GCT ACA -3'	
5'- CCT TCT GGG TTC TGC TTC TC -3'	5'- CAA CAA AAT TTG GGG CTA ACA -3'	

Supporting Online Methods:

SNP detection by restriction enzyme digestion of PCR amplicons.

The variants of the H2K gene (MHC class I antigens) were amplified by PCR. Exon-spanning oligonucleotides were designed in order to flank restriction site variants for *BsiE*1 (specific for H-2K**b**). The sense oligonucleotide (CCTGGGCTTCTACCCTGCT) is located in exon 4, the anti-sense primer (CCACCACAGCTCCAGTGAC) in exon 5 of the H-2K gene. PCR was carried out with 50ng genomic DNA. PCR reactions were set up in a total volume of 50 µl reaction mix containing 2 units of AmpliTaq DNA polymerase (Applied Biosystems [Perkin Elmer], Weiterstadt, Germany). PCR cycling was performed using the following protocol: 94 C for 4 min (initial denaturation); 92 C for 40 sec, annealing 60 C for 40 sec, 72 C for 40 sec (35 cycles); 72 C for 10 min (final elongation). PCR products were purified using Qiaquick PCR purification kit (Qiagen, Valencia, CA, USA). Purified PCR products were digested with *BsiE*1 (NEB, Beverly, MA, USA) for 8 hours, and loaded on an agarose gel (Cambrex BioScience Rockland, 50180). Lane 1: 100bp size marker, lane 2: uncut PCR product, lane 3: uncut spiked DNA, lane 4: C57BL/6 *BsiE*I digested, lane 5: CBA *BsiE*I digested, lane 5-13: nine p(MII)ES cells from B6CBAF1 mice *BsiE*I digested, lane 14-18: five p(MI)ES cells from B6CBAF1 mice *BsiE*I digested. As internal controls for the completion of restriction enzyme digestions, we spiked in a DNA fragment (arrow) containing *BsiE*I restriction enzyme sites, to indicate complete digestion. Spiked DNA was made by PCR amplification of puc19 plasmid using the primer set, CCTCCGATCGTTGTCAGAAG and CTGGCGTAATAGCGAAGAG.

The variants of the Tap1 gene were amplified by PCR using the primer set, AAGAGCACCGTGGCTGCC and GTGCAGGTAATGATGATCATA. PCR was carried out with 50ng genomic DNA. PCR reactions were set up in a total volume of 50 µl reaction mix containing 2 units of AmpliTaq DNA polymerase (Applied Biosystems [Perkin Elmer], Weiterstadt, Germany). PCR cycling was performed using the following protocol: 94 C for 4 min (initial denaturation); 92 C for 30 sec, annealing 55 C for 30 sec, 72 C for 60 sec (35 cycles); 72 C for 10 min (final elongation). PCR products were purified using Qiaquick PCR purification kit (Qiagen, Valencia, CA, USA). Purified PCR products were digested with *Hha*1 (NEB, Beverly, MA, USA) for 8 hours, and loaded into agarose gel (Cambrex BioScience Rockland, 50180). Lane 1: 100bp size marker, lane 2: uncut PCR product, lane 3: uncut spiked DNA, lane 4: spiked DNA *Hha*I digested, lane 5: C57BL/6 *Hha*I digested, lane 6: CBA *Hha*I digested, lane 7: B6CBAF1 *Hha*I digested, lane 8-13: six MHC-matched p(MI)ES cells from B6CBAF1 mice *Hha*I digested, lane 14: 100bp size marker. As internal controls for the completion of restriction enzyme digestions, we spiked in a DNA fragment containing *Hha*I restriction enzyme sites, to indicate complete digestion.

SNP genotyping by DNA sequencing.

Primers used in this study (Chromosome number: distance from centromere (bp)) are listed in Table S1. PCR was carried out with 50ng genomic DNA. PCR reactions were set up in a total volume of 50 μl reaction mix containing 2 units of AmpliTaq DNA polymerase (Applied Biosystems [Perkin Elmer], Weiterstadt, Germany). PCR cycling was performed using the following protocol: 94 C for 4 min (initial denaturation); 92 C for 40 sec, annealing 60 C for 40 sec, 72 C for 40 sec (35 cycles); 72 C for 10 min (final elongation). PCR products were purified using Qiaquick PCR purification kit (Qiagen, Valencia, CA, USA). The DNA sequence analysis with the purified PCR products was performed by the Molecular Genetics Core Facility –Boston Children's Hospital-Harvard Medical School.

Genome-wide SNP genotyping.

Genotyping was performed at the Broad Institute NCRR Center for Genotyping and Analysis using the Illumina multiplexed allele extension and ligation method (Golden Gate) with detection using oligonucleotide probes covalently attached to beads which are assembled into fiber optic bundles (Bead Array) .

p(MII)ES cell derivation.

Hybrid B6CBAF1 mice (C57BL/6 x CBA) (Jackson Laboratories) were used as oocyte donors. Eight to ten week old female mice were superovulated by injection of 5 IU Pregnant mare serum gonadotropin (PMSG, Calbiochem 367222) and 48 h later, 5 IU Human chorionic gonadotropin (hCG, Calbiochem230734). Oocytes were collected 14 –15 hours after hCG injection. Oocytes with cumulus cells were activated in KSOM (Specialty Media, MR-106-D) containing 10 μM calcium ionophore A23187 (Sigma, C7522) for 5 min in air, then in 2 mM 6-dimethylaminopurine (6-DMAP) (Sigma, D2629) and 5 μg/ml of cytochalasin B (Sigma, C6762) dissolved in KSOM at 37˚C in 5% CO2 for 3 hours. Embryos were then washed five times in 500 microliters of KSOM. Embryos were cultured in KSOM. All cultures were performed at 37˚C in 5% CO2, 5% O2, and 90% N2. Two and four days after activation stages and rate of embryo development evaluated under a stereomicroscope. The zona pellucida of the blastocysts were removed in 1% pronase in FHM mdia (Specialty Media, MR-024-D), and cells were cultured in the presence of MEF in serum free ES maintenance media (Gibco, 10829-018) with 50 μM MAP kinase inhibitor PD98059 (Cell Signaling Tech, #9900) in 5% CO2, 5% O2, and 90% N2. Developmental stage was evaluated under a stereomicroscope.

p(MI)ES cell derivation.

Eight to ten week old female mice were superovulated by injection of 5 IU PMSG, and 48 h later, 5 IU hCG. Oocytes were collected from ovary within 9 hours after hCG injection. Cumulus cells were dispersed by incubation in hyaluronidase (Sigma, H4272: 1mg/ml in KSOM) for 2-5 minutes at 37ºC for 5 min. Cumulus-free oocytes were then washed five times in 500 microliters of KSOM. The cumulus cell free oocytes were incubated in KSOM containing 5 μg/ml of cytochalasin D (Sigma, C8273) for 3 hours. Cumulus-free oocytes were then washed five times in 500 microliters of KSOM and incubated in KSOM at 37°C in 5% CO2 for 6 hours. The oocytes were activated in KSOM containing 10 μM calcium ionophore A23187 for 5 min in air, then in 2 mM 6-dimethylaminopurine (6-DMAP) (Sigma, D2629) dissolved in KSOM at 37°C in 5% CO2 for 3 hours. Embryos were then washed five times in 500 microliters of KSOM. All cultures were performed in culture condition at 37°C in 5% CO2, 5% O2, and 90% N2 with 50 μM MAP kinase inhibitor PD98059 (Cell Signaling Tech, #9900) in serum free ES maintenance media, which enhanced ES cell isolation efficiency. Developmental stage was evaluated under a stereomicroscope.

Teratoma induction

We assayed teratoma formation by undifferentiated ES cells by injecting 106 cells into the subcutaneous tissue above the rear haunch of 6 week old mice. Teratomas were analyzed six to twelve weeks post-injection. We assayed teratoma formation from pre-differentiated ES cells by injecting 14 day old embryoid bodies containing 2 x 106 live-cells into the subcutaneous tissue above the rear haunch of 6 week old mice. The live-cells were determined by Trypan Blue Vital Staining (Sigma, T8154) after dissociating the EBs with collagenase (*6*). Teratoma formation was monitored for 3 months post injection.

Statistical analysis.

Table 2. We tested the hypothesis that ES cells genetically matched to the recipient's MHC profile will form teratomas, while those with any degree of MHC mis-match will not. Both controls (experiments with fES cells) and test samples (experiments with pES) agree with the hypothesis ($p < 0.001$). Differences between the control and test samples were evaluated by Chi-Square analysis incorporating Yates' correction for continuity. The value of Chi-Square (1.0456, with 1 d.f.) is smaller than the critical value at the 0.05 level of significance, which is 3.841. We therefore conclude that the teratoma formation frequencies within the pES test samples follow the hypothesis and do not significantly differ from the control fES samples, as would be expected by chance.

References

1. S. H. Klebs, M. W. Hoffmann, P. B. Musholt, B. Bayer, T. J. Musholt, *J Immunol Methods* 276, 197 (May 1, 2003).
2. The-Jackson-Laboratory, www.informatics.jax.org (2006).
3. S. Bao *et al.*, *Hum Reprod* 17, 1311 (May, 2002).
4. J. R. Mann, I. Gadi, M. L. Harbison, S. J. Abbondanzo, C. L. Stewart, *Cell* 62, 251 (Jul 27, 1990).
5. B. J. Yoon *et al.*, *Nat Genet* 30, 92 (Jan, 2002).
6. N. Geijsen *et al.*, *Nature* 427, 148 (Jan 8, 2004).

Children's Hospital Boston

International Visitors | Request an Appointment | Directions

Search this site advanced search GO

ABOUT US FIND A SPECIALIST LOCATIONS CAREERS NEWS ROOM GIVING TO CHILDREN'S

Clinical Services | For Patients & Families | For Health Professionals | Research

My Child has: condition or treatment GO

News Room

« back

- News Room
- News Releases
  - Archive 2010
  - Archive 2009
  - Archive 2008
  - Archive 2007
  - Archive 2006
  - Archive 2005
  - Archive 2004
  - Archive 2003
  - Archive 2002
  - Archive 2001
  - Archive 2000
- Embargoed News Releases
- Resources for Reporters
- Backgrounders
- Publications
- Sign up for Newsletters & News Releases
- News Clips
- Videos
- Sala de Noticias

Search News Room

Search News Room only

GO

Email this Page

> Home > News Room > News Releases > Discredited Korean stem cells' true origins revealed

Discredited Korean stem cells' true origins revealed

DNA analysis finds they were the world's first human embryonic stem cells derived from eggs alone

August 2, 2007

A report from researchers at Children's Hospital Boston and the Harvard Stem Cell Institute sheds new light on a now-discredited Korean embryonic stem cell line, setting the historical record straight and also establishing a much-needed set of standards for characterizing human embryonic stem cells. The report was published online August 2 by the journal *Cell Stem Cell*.

George Daley, MD, PhD

In 2004, Korean investigators announced the creation of the world's first human embryonic stem cells through somatic cell nuclear transfer, entailing transfer of genetic material from a cell in the body into an egg. Now, research led by Kitai Kim, PhD, and George Q. Daley, MD, PhD, of the Children's Hospital Boston Stem Cell Program demonstrates that the Koreans unwittingly created something entirely different--the world's first human embryonic stem cell to be derived by parthenogenesis, a process that creates an embryo containing genetic material only from the donor egg.

"We know now that the Koreans' first supposed nuclear transfer-derived stem cell line was actually derived from the woman's egg alone," Daley says.

The Koreans' 2004 paper, published in Science, was retracted by the journal in early 2006 amid evidence that researchers Hwang Woo-Suk et al. had falsified their data. An initial investigation of the Korean group's first embryonic stem cell line suggested it might be parthenogenetic in origin, but the analysis was inconclusive, and the cells' origin, until now, had never been fully explained in a peer-reviewed journal.

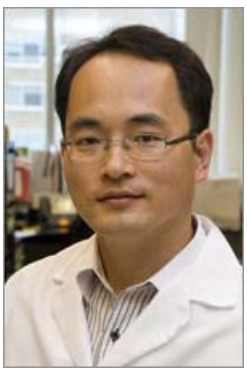

Kitai Kim, PhD

Kim, Daley and collaborators used sophisticated genetic techniques to compare mouse embryonic stem cells derived from different sources: from embryos produced by natural fertilization; from embryos produced by parthenogenesis (through artificial activation of unfertilized eggs); and from embryos created through somatic cell nuclear transfer (replacing the nucleus of an egg with the nucleus from a cell in the body). They also tested three human embryonic stem cells isolated from fertilized embryos as well as the Korean line of human cells claimed to have been created through nuclear transfer.

They discovered that parthenogenetic embryonic stem cells have a distinct genetic signature that reflects their biological origins. All cells typically contain paired sets of chromosomes,

Additional Resources

George Daley, MD, PhD

- Research profile
- Clinical profile
- The Daley Laboratory

Video from an interview with Dr. Daley

Stem Cell Program at Children's Hospital Boston

George Daley, ISSCR president

one inherited from the mother and the other from the father. During the process of parthenogenesis, one set of chromosomes is duplicated, resulting in both chromosomes of the pair being of one parental type or the other (a pattern called homozygosity, which has reduced genetic diversity). Kim and Daley showed previously that because chromosomes often exchange genetic material early in the process of cell division that creates the egg (meiosis), the duplicated chromosomes are not actually identical, but have places where the genes differ between members of the pair (called heterozygosity). In embryonic stem cells of parthenogenetic origin, this occurs especially toward the ends of the chromosomes, which are more likely to exchange genetic material, rather than the middle. In contrast, embryonic stem cells created through nuclear transfer show a consistent pattern of variation through all regions of the chromosome -- thus making them easily distinguishable from parthenogenetic cells.

The Korean cell line displays a genetic pattern that is clearly consistent with a parthenogenetic origin, Kim and Daley now show.

Because mistakes during nuclear transfer can result in parthenogenetic cells, Daley believes that the Hwang group generated parthenogenetic stem cells by accident, and didn't have the tools to conclusively determine what they had created. The first isolation of parthenogenetic stem cells from humans would have been an important contribution, but the Hwang group's attempt to pass off the cells as made by nuclear transfer was instead "a woeful case of misconduct," he says.

Parthenogenesis is a method of reproduction, common in plants and in some animals, in which the female can generate offspring without the contribution of a male. Daley's group has been stimulating parthenogenesis in the laboratory as a way of creating customized embryonic stem cells that can treat disease without being rejected by the immune system.

The team recently demonstrated in mice a feasible technique for generating parthenogenetic embryonic stem cells that were genetically matched to the egg donor at the genes that control tissue typing, and are attempting to create similar cells from humans. (See News Release).

Daley, who is a member of the executive committee of the Harvard Stem Cell Institute and president of the International Society for Stem Cell Research, notes that scientists now have two powerful tools: human parthenogenesis, which appears to be an efficient means of producing human embryonic stem cells, and genetic screening, which can be used to scan stem cells and help define their origins.

Daley imagines a future in which scientists could create a master bank of parthenogenetic embryonic stem cells with genetically selected cells that could be matched to patients on the genes that control immune rejection. Having all the genetic material come from the mother, as it does in parthenogenesis, reduces tissue compatibility issues.

"There has been an advance in the idea that you can couple parthenogenesis and genetic screening to identify those cell lines that are going to be most helpful," Daley says.

Parthenogenetic embryonic stem cells do not obviate the need to also create embryonic stem cells through nuclear transfer or from human embryos, he adds. "Each of the strategies has its own applications, and there are certain types of research and certain fundamental questions--and major areas of therapy--that can only be accomplished with these other types of stem cells," Daley says.

The work was supported by private philanthropic funds of Children's Hospital Boston and the Harvard Stem Cell Institute, and was performed with collaborators at the Memorial Sloan Kettering Cancer Institute (NY), University of Cambridge (UK), Riken Kobe (Japan), and the Whitehead Institute (MA).

Contact:
Elizabeth Andrews
617-355-6420
elizabeth.andrews@childrens.harvard.edu

Children's Hospital Boston is home to the world's largest research enterprise based at a pediatric medical center, where its discoveries have benefited both children and adults since

1869. More than 500 scientists, including eight members of the National Academy of Sciences, 11 members of the Institute of Medicine and 10 members of the Howard Hughes Medical Institute comprise Children's research community. Founded as a 20-bed hospital for children, Children's Hospital Boston today is a 347-bed comprehensive center for pediatric and adolescent health care grounded in the values of excellence in patient care and sensitivity to the complex needs and diversity of children and families. Children's also is the primary pediatric teaching affiliate of Harvard Medical School. For more information about the hospital and its research visit: : www.childrenshospital.org/newsroom.

- ### -

Children's Hospital Boston | Harvard Medical School Children's Hospital Boston is the primary pediatric teaching hospital of Harvard Medical School

Contact Us Site Map Privacy Accessibility Give Now en Español